Marine Geology 266 (2009) 182–197

Contents lists available at ScienceDirect

Marine Geology

journal homepage: www.elsevier.com/locate/margeo

Late Glacial–Holocene climate variability at the south-eastern margin of the Aegean Sea

M.V. Triantaphyllou [a,*], P. Ziveri [b,c], A. Gogou [d], G. Marino [c], V. Lykousis [d], I. Bouloubassi [e], K.-C. Emeis [f], K. Kouli [a], M. Dimiza [a], A. Rosell-Melé [c], M. Papanikolaou [g], G. Katsouras [d,h], N. Nunez [c]

[a] University of Athens, Faculty of Geology and Geoenvironment, Dept. of Historical Geology-Paleontology, Panepistimiopolis 15784, Athens, Greece
[b] Dept. of Paleoclimatology and Geomorphology, FALW, Vrije Universiteit Amsterdam, The Netherlands
[c] ICTA, Autonomous University of Barcelona (UAB) Edifici Cno-Campus UAB, 08193 Bellaterra, Spain
[d] Hellenic Centre for Marine Research, Inst. of Oceanography, 19013 Anavyssos, Greece
[e] Laboratoire d'Océanographie et du Climat: Expérimentation et Approche Numérique, Université Pierre et Marie Curie, Paris Cedex 05, France
[f] Institut für Biogeochemie und Meereschemie, Universitat Hamburg, Bundesstr. 55, 20146 Hamburg, Germany
[g] University of Cambridge, Department of Geography, Cambridge Quaternary, CB2 3EN Cambridge, UK
[h] University of the Aegean, Dept. of Marine Sciences, 81100 Lesvos, Greece

ARTICLE INFO

Article history:
Received 25 July 2008
Received in revised form 23 June 2009
Accepted 6 August 2009
Available online 15 August 2009

Communicated by G.J. de Lange

Keywords:
coccolithophores
pollen
benthic foraminifera
biomarkers
alkenone-based SST
sapropel S1
sapropel-like layer SMH

ABSTRACT

New micropaleontological, palynological, and geochemical results from a relatively shallow (~500 m) sediment core (NS-14) in the south-eastern Aegean Sea provide a detailed picture of the regional expression of sapropel S1 formation in this sub-basin of the eastern Mediterranean Sea. Specifically, freshwater input during ~10.6–10.0 ka BP has preceded the deposition of S1. Further decrease in surface water salinity is evidenced between 10.0 and 8.5 ka BP at the lower part of S1a, which in respect to S1b, is featured by warmer (~19.5 °C) and more productive surface waters associated with dysoxic bottom conditions. A series of coolings detected within the S1 depositional interval, may be linked to outbursts of cold northerly air masses and relevant pulses in the deep-intermediate water ventilation that caused the S1 interruption between 7.9 and 7.3 ka BP and culminated during the deposition of S1b, with the decline of deep chlorophyll maximum (DCM) at ~6.5 ka BP. The climate instability and the relevant absence of anoxia weakened the organic matter preservation in the shallow south-eastern Aegean margin during the S1 times. NS-14 record provides evidence for a distinct mid Holocene warm (up to ~25 °C) and wet phase associated with the deposition of the sapropel-like layer SMH (Sapropel Mid Holocene), between 5.4 and 4.3 ka BP. The SMH layer could represent evidence of on-going, albeit weak, African monsoon forcing, only expressed at the south-eastern edge of the Aegean Sea. Its end is associated with the 4.2 ka BP Northern Hemisphere mega-drought event and the termination of the African Humid Period at 3.8 ka BP.

1. Introduction

The eastern Mediterranean is an efficiently ventilated and highly evaporative semi-enclosed sea with surface waters depleted in phosphate, nitrate and silicate, and low biological production (Krom et al., 1992; Tselepides et al., 2000). However, the (quasi)periodic occurrence of organic-rich layers, so-called sapropels, throughout the sedimentary record of the last 13.5 million years (Hilgen et al., 2003), points to the development of dramatically different oceanographic and trophic conditions in the past (for extensive reviews see, e.g., Rohling, 1994; Cramp and O'Sullivan, 1999; Emeis et al., 2003). The accepted paradigm for sapropel formation dictates that these deposits formed under deep-sea anoxic/dysoxic conditions, which developed in concert with distinct minima in the orbital precession cycle, i.e., every ~21,000 years (Rossignol-Strick et al., 1982; Hilgen, 1991; Lourens et al., 1992, 1996). Briefly, the precession driven intensifications of the boreal African monsoon fuelled enhanced freshwater discharge along the North African margin of the eastern Mediterranean (e.g., Rohling et al., 2002a; Scrivner et al., 2004; Ehrmann et al., 2007). These positive shifts of the basin's freshwater budget – likely supplemented by contemporaneous increases in the freshwater supply from the southern European margin (Kotthoff et al., 2008) – inhibited the convective deep water formation processes, in turn, leading to oxygen starvation in the deep sea (Rohling, 1994; de Lange et al., 2008). Emeis et al. (2000, 2003) also emphasized the role of the sea surface warming during intervals of precession minima, which may have intensified the surface buoyancy gain, thereby contributing to weaken the deep water circulation. While there exists ample consensus on the enhanced preservation of organic matter under oxygen-deficient conditions of the eastern Mediterranean bottom waters

* Corresponding author. Tel.: +30 210 7274893.
E-mail address: mtriant@geol.uoa.gr (M.V. Triantaphyllou).

0025-3227/$ – see front matter © 2009 Elsevier B.V. All rights reserved.
doi:10.1016/j.margeo.2009.08.005

(De Lange et al., 1999, 2008; Moodley et al., 2005), other studies emphasize that an increase in the export productivity from the pelagic layer may have played a critical role in the sapropel formation (e.g. De Lange and Ten Haven, 1983; Kemp et al., 1999; Mercone et al., 2001).

It has been found that the precession driven changes in the eastern Mediterranean water column have led to different sedimentary features in the individual sub-basins (Emeis et al., 2000). Much interest has recently been centred on the Aegean Sea (Rohling et al., 2002b; Casford et al., 2002, 2003, 2007; Ehrmann et al., 2007; Kuhnt et al., 2007; Marino et al., 2007), because it represents an important area of deep water formation for the entire eastern Mediterranean (Zervakis et al., 2004), which appears particularly sensitive to climate forcing today (Roether et al., 1996; Theocharis et al., 1999; Zervakis et al., 2000) as well as in the past (Kuhnt et al., 2007; Marino et al., 2007). Importantly, by virtue of its location, at the north-eastern sector of the Mediterranean, in winter the Aegean Sea is under the direct influence of northerly winds (Poulos et al., 1997), thereby holding great potential as key sedimentary archive to investigate the response of the regional climate to past high-latitude forced climate fluctuations. Indeed, several recently generated Aegean paleoceanographic records suggest that – during the Holocene – short-term cooling episodes, which are bound to the strengthening of northerly winds, are superimposed on the underlying subtropical/tropical control of the regional hydrography and ecosystems (Rohling et al., 2002b; Casford et al., 2003; Gogou et al., 2007; Marino, 2008). These findings suggest that during the Holocene the eastern Mediterranean climate was less stable than previously thought.

The present study investigates an expanded sediment record covering the last ~13 ka BP, from the shallow south-eastern margin of the Aegean Sea. We use a combined coccolithophore, pollen, benthic foraminifera, and organic geochemistry proxy data to address three main questions: (*1*) what is the fingerprint of the northern hemisphere climate variability on the south-eastern Aegean climate? (*2*) what is the interaction between primary production and organic matter preservation at intermediate depths during sapropel S1 deposition? (*3*) what are the major changes in sea surface temperature, hydrography, primary production, and in the regional moisture availability in the period immediately following the deposition of sapropel S1?

2. Basin location and oceanographic setting

The Aegean Sea, which is situated between Turkey and Greece (Fig. 1A), is connected with the Black and Marmara Seas through the Dardanelles Straits, and with the open eastern Mediterranean (Levantine Sea) through the Cretan Straits. The cooler (9–22 °C) and lower salinity (24–28 psu) Black Sea outflow waters flows along the east coast of Greece to reach the southwest Aegean Sea, and, due to their high nutrient contents, fuel productivity in the North Aegean Sea (Lykousis et al., 2002). The warm (16 °C in winter; 25 °C in summer) and saline (39.2–39.5 psu) Levantine surface waters flow northward along the eastern Aegean to the Dardanelles Straits (Zervakis et al., 2000, 2004). Several rivers discharge into the Aegean Sea, mostly from the north Hellenic coast and from the east coast of Turkey (Fig. 1A). Together, Black Sea outflow waters and river inputs both supply the Aegean with freshwater (Poulos et al., 1997; Roussakis et al., 2004).

Regarding the subsurface circulation, between 70 and 400 m depth, the Aegean is filled by the Levantine Intermediate Water mass (LIW). Between 400 and 900 m in the South Aegean can be identified a salinity minimum, which reflects the Transitional Mediterranean Water mass (TMW) (Lykousis et al., 2002). The development of deep convection takes place during the winter season due to favourable weather and hydrographic conditions, which are strongly affected by northerly outbreaks of cold and dry polar/continental air (Poulos et al., 1997; Theocharis et al., 1999). Deep convection leads to an increased oxygenation of the intermediate and deep layers. Overall, the distribution of oxygen (and nutrients) in the South Aegean Sea is influenced by the exchange of water masses through the Cretan Straits. In the Southern Aegean Sea sediments, oxygen penetration extends to about 3–5 cm (Lykousis et al., 2002). The South Aegean sub-basin is considered as a "typical oceanic margin" environment, characterised by very low export rates of organic matter from the euphotic zone (mean annual flux at 200 m: 5.6 mg m^{-2} d^{-1}; Stavrakakis et al., 2000) and organic — poor sediments, with mean total organic carbon values of 0.34% (Lykousis et al., 2002).

3. Material and age model

3.1. Core description

Core NS-14 was taken during the R/V Aegaeo-Cruise 1998, in western Kos basin (Fig. 1B), from a water depth of 505 m at 36°38′55″N and 27°00′28″E. Gray coarse sands with pebbles prevail from the core bottom (400 cm) to 300 cm. Between 300 cm and the core top the sediment mainly consists of gray hemipelagic mud (Fig. 2A). At 240 to 231 cm, we found a turbiditic layer (T) with graded bedding and abundant shallow benthic foraminiferal microfauna (mainly *Quinqueloculina* spp.). The dark gray to olive gray mud of sapropel S1, which occurrence is also confirmed by the total organic carbon (TOC) profile (see Section 5.1), extends from 120 to 55 cm. The S1 layer is divided into two sub-units (hereafter termed S1a and S1b, respectively), which are separated by an 11 cm thick (from 80 to 69 cm) lighter gray interval, here interpreted as the S1 interruption (Fig. 2A). Another dark olive gray mud sapropel-like layer, which we name Sapropel Mid Holocene (SMH); see Section 6.3) occurs between 40 and 25 cm. The most recent Z2 Santorini ash layer is positioned at 17 cm depth.

3.2. Chronology

Seven accelerator mass spectrometry (AMS) radiocarbon (^{14}C) datings (Table 1; Fig. 2B) were performed at the laboratories of Beta Analytic (USA) on cleaned, hand-picked mixed benthonic and planktonic foraminifera from core NS-14. Dating mono-specific planktonic assemblages was not possible due to relatively low amounts of planktonic foraminifera in core NS-14. However, due to the location of core NS-14, it is rather unlikely that this approach will considerably affect the precision of the chronology adopted in our study. In fact, the vigorous upwelling of intermediate waters to the surface along the south-eastern Aegean margin (Lascaratos, 1992; Yüce, 1995) imply a well homogenized water column and thus fairly small age offsets between surface and bottom waters in this sector of the basin.

Conventional ^{14}C ages have been calibrated using the program CALIB 5.0.2 (Stuiver and Reimer, 1993; Stuiver et al., 1998) with a regional reservoir age correction (ΔR) of 149 ± 30 years for sapropel interval (Facorellis et al., 1998) and 58 ± 85 outside the sapropel (Reimer and McCormac, 2002). In order to reduce the bias towards older ages produced by the contribution of old carbon (Casford et al., 2007) and by the presence of benthic foraminiferal shells in the dated material, we base the NS-14 chronology on the youngest ages of the age range provided by this calibration exercise.

AMS ^{14}C datings at 393 cm and 344 cm (Table 1) provided virtually identical ages. Taken at face value these dates would imply disproportionally high sedimentation rates in this segment of the record. However, the entire interval below 300 cm consists of olive gray coarse sands, which are likely reflective of a sediment gravity flow event at ~18 ^{14}C ka BP. Accordingly, these deposits either derive from a turbidite event during the early stages of the last deglaciation (Roussakis et al., 2004), or from seismically induced landslide phenomena (Papanikolaou and Nomikou, 2001). Hence, dating points at 393 and 344 cm were not considered here for chronological purposes. The Minoan Santorini ash layer (Z2 in Fig. 2A) was used as an additional time marker (3550–3577 yr cal. BP; Friedrich et al., 2006).

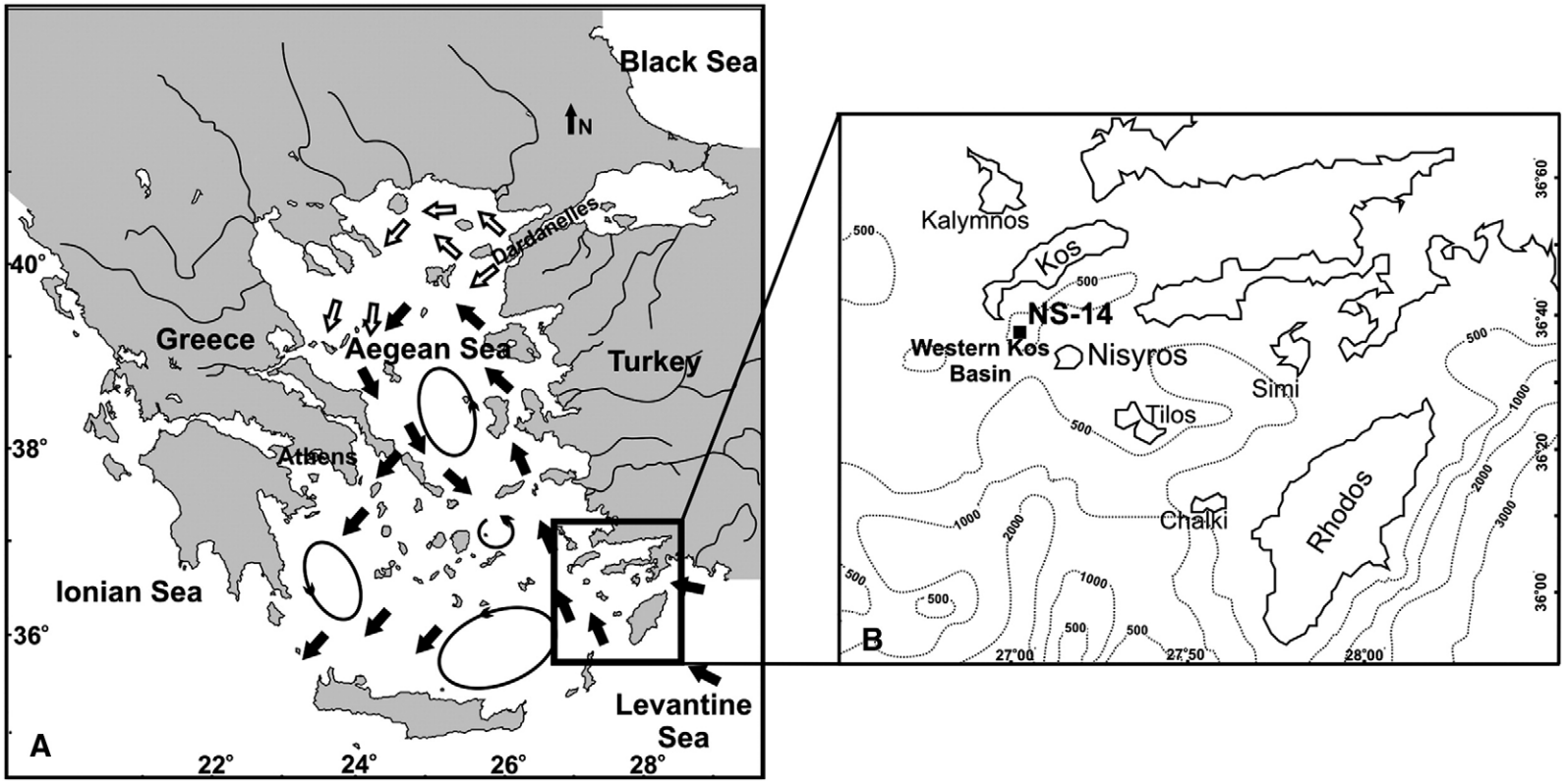

Fig. 1. Location map of the study area in the south-eastern Aegean Sea.

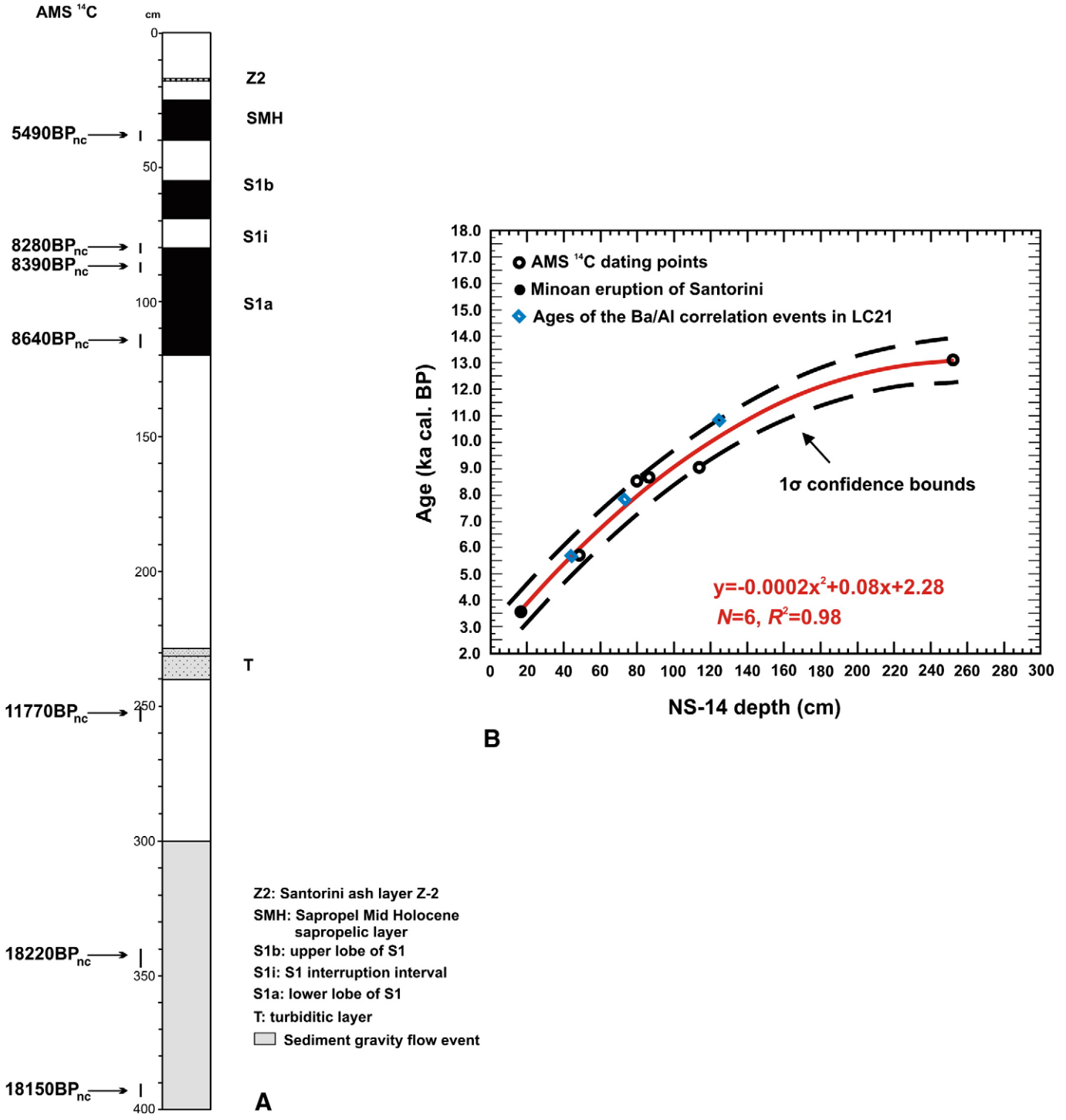

Fig. 2. (A). Core NS-14 stratigraphy. (B). Age model of the chronology for core NS-14. Solid red line is the 2nd order polynomial fit through both the five youngest calibrated AMS 14C datings (open dots) and the age of the ash layer produced by Minoan eruption of Santorini (solid dot) (Friedrich et al., 2006). Open blue diamonds represent the ages of the base, saddle and top of the NS-14 Ba/Al anomaly in the robust chronological framework recently proposed by Casford et al. (2007) for nearby core LC21. (For interpretation of the references to colour in this figure legend, the reader is referred to the web version of this article.)

Chronology adopted in this study for core NS-14 derives from a polynomial fit through the five calibrated AMS ^{14}C datings mentioned above and the time marker correlative to the Minoan eruption of Santorini (Fig. 2B). The 1σ uncertainty associated to this exercise is ±0.71 kyr. We tested the NS-14 chronology against the multi-proxy chronological framework recently proposed by Casford et al. (2007) for a generous number of sediment cores from the Aegean Sea, thereby supporting the robustness of our chronology. By transferring the ages proposed by Casford et al. (2007) for the onset, saddle, and termination of the Ba/Al anomaly onto the NS-14 chronological framework we note that these points fall all within the 1 σ bounds of the polynomial fit in Fig. 2B. Hereafter ages will be discussed as ka BP.

4. Methods

Core NS-14 was sampled at 2 cm spacing throughout with the exception of the sapropel layers, where sampling was carried out at higher, 1 cm resolution. Samples were then sub-sampled for benthic

Table 1
Age model pointers for the investigated core NS-14.

Depth (cm)	AMS Lab code[a]	Conventional ^{14}C age (yr) ± 1σ error	Calibrated ^{14}C age (yr)[b]	1σ age range
17			3563.50[c]	1600–1627[c]
48		5490 ± 40	5698	5698–5904
80		8280 ± 50	8515	8515–8706
86		8390 ± 40	8670	8670–8885
114		8640 ± 40	9022	9022–9190
252		11770 ± 60	13101	13101–13273
344		18220 ± 90	20733	20733–21186
393		18150 ± 90	20640	20640–21084

[a] Beta Analytic, Inc., Miami, FL, USA.
[b] Conventional 14C ages were converted into calibrated ages by using Calib vs. 5.0.2 software (Stuiver et al., 1998) and the MARINE04 calibration dataset. Local ΔR corrections were applied; ΔR = 58 ± 85 years outside the sapropel (Reimer and McCormac, 2002) and ΔR = 149 ± 39 years in the sapropel (Facorellis et al., 1998).
[c] Age of the Minoan eruption of Santorini (Friedrich et al., 2006).

foraminifera, coccolithophore, pollen, and geochemical analyses. Mean sample resolution for geochemical analyses in the uppermost part of the core, and for benthic foraminifera census counts through the upper 145 cm were performed at a mean samples resolution of 6 and 5 cm respectively, has been used for benthic foraminiferal analysis. All other analyses have been performed till 220 cm depth from the core top.

4.1. $CaCO_3$, TOC and Ba/Al ratio analyses

Total organic carbon (TOC) concentrations were determined in 58 freeze dried and homogenized samples using a Thermo 1500 elemental analyser. The concentrations of calcium carbonate were determined on the same samples using a coulometer after liberation of CO_2 with 2 N HCl. Total concentrations of Al (%Al_2O_3) and Ba (ppm) were calculated in 62 samples by X-ray fluorescence spectrometry on fused discs. Relative precision is better than ±2% for carbon and ±5 for Ba and Al.

4.2. Coccolithophore analyses

For coccolithophore analysis the preparation of 131 samples followed the standard smear slide techniques. For detailed descriptions of the quantitative methods and taxonomy we refer to Negri and Giunta (2001), Giunta et al. (2003), Principato et al. (2006). Results are based on a total of (at least) 300 counted specimens per sample, and are presented in relative abundances in order to avoid any dilution effects of, e.g. terrigenous matter input (Flores et al., 1997).

In order to evaluate primary production, the depth of the nutricline, and stratification in the water column we have used the relative amounts of *Florisphaera profunda* (Beaufort et al., 1997). The lower photic zone species *F. profunda* (Okada and Honjo, 1973) is a very reliable proxy to reconstruct the depth of the nutricline–thermocline (Molfino and McIntyre, 1990), and high relative abundances of this taxon indicate high stratification of the water column and low productivity in the surface layer (e.g. Castradori, 1993; Beaufort et al., 1997, 2001; Flores et al., 2000). The comparison between *F. profunda* percentages and primary production from satellite imagery has allowed quantitative estimates of past primary production fluctuations in the Indian Ocean (Beaufort et al., 1997, 2001) and the central Mediterranean Sea (Incarbona et al., 2008). In the present study we have used the equation proposed by Incarbona et al. (2008) for the estimation of the net primary production (NPP), NPP = 885.864 + (−138.963 * ln (*F. profunda* %)), as this has been provided by comparison of satellite primary production from North Sicily Strait, which is relatively close to our study area. In addition, we have established the use of the ratio between *Florisphaera profunda* (F) and *Emiliania huxleyi* (E) abundances: $S = F/F + E$ as stratification index, (modified from Flores et al., 2000). *F. profunda* and *E. huxleyi* generally in the Mediterranean are the dominant coccolithophores in the lower and upper photic zone. In particular, the increase of *F. profunda* vs. the high surface nutrient indicator (Young, 1994) *E. huxleyi*, a species that prevails in the Aegean surface waters mainly in winter/spring (Triantaphyllou et al., 2004; Dimiza et al., 2008), suggests high values of *S*. The increase in *S* values indicates gradual establishment of stratified conditions in the water column related either to warm conditions or fresh water input, and the onset of a nutrient-rich environment in the deep photic zone. The abundances of *Helicosphaera* spp. (mainly *H. carteri*) together with *Braarudosphaera begelowii* have been used as indicators of salinity decrease (Flores et al., 1997; Colmenero-Hidalgo et al., 2004; Negri and Giunta, 2001).

4.3. Palynological processing

For pollen analysis, 88 oven-dried sediment samples were spiked with *Lycopodium clavatum* spores, weighted, and treated with 10% HCl and 38% HF and eventually sieved over a 10 μm sieve. A minimum of 150 pollen grains was counted per sample. The ratio $H = AP/St$ (AP: Arboreal taxa excluding *Pinus*, which was it was considered over-represented in the spectra; St: Steppic taxa including *Artemisia*, Chenopodiaceae, Compositae and Poaceae), has been used as a humidity index (Bottema, 1991; Vermoere et al., 1999). Mediterranean taxa include *Olea* and *Pistacea*. The concentration of aquatic palynomorphs (taxa living in rivers and lakes like *Sparganium*, *Pediastrum* and Zygnemantaceae) has been used as a proxy of river runoff into the basin (Targarona, 1997).

4.4. Benthic foraminiferal analyses

Thirty sediment samples for benthic foraminiferal census counts were approximately 2 g dry weight each. They were soaked in distilled water and wet sieved over 63 and 150 μm sieves. Residues were dried at 50 °C and census counts were performed on the 150 μm fraction. Relative abundances of benthic foraminifera are presented and discussed in this study.

4.5. Organic geochemistry

The determination of lipid biomarkers was carried out on 57 samples. Lipids were extracted from freeze-dried sediments by ultrasonication using a mixture of dichloromethane/methanol (4:1) and separated into different compound classes on silica gel column chromatography, using solvent mixtures of increasing polarity (see Gogou et al., 2007). Individual compounds were identified and quantified by GC–FID and GC–MS with a combination of comparison of GC-retention times to authentic standards and comparison of their mass-spectral data to those in the literature. Sums of selected C_{27} and C_{28} methyl-sterols and C_{30} desmethyl sterols (presented as marine sterols), long chain alkenones with 37 and 38 carbon atoms, of the isoprenoid derivatives loliolide and isololiolide and the most abundant long chain *n*-alkanols *n*-C_{26}, *n*-C_{28} and *n*-C_{30} of terrestrial origin (presented as Ter-alkanols) were calculated following Gogou et al. (2007). Biomarkers exhibit different resistance to early diagenesis and under oxic/dysoxic conditions in the marine environment, so their use as paleoproductivity proxies should be done with caution (Versteegh and Zonneveld, 2002). Despite this limitation, the detailed study of a variety of lipid classes still enables the recognition of the major sources contributing to the sedimentary organic matter – both autochthonous and allochthonous – and permits assessment of the transformation processes/diagenetic pathways of organic matter in paleoceanographic studies (Hinrichs et al., 1999; Menzel et al., 2002, 2003; Gogou et al., 2007). Estimates of past sea surface temperature (SST) were made on 62 samples by means of the unsaturation ratios of alkenones ($U^{k'}_{37}$) and the global calibration given by

Muller et al. (1998). The analytical precision based on multiple extractions of sediment samples was better than 0.6 °C. Note that this error refers to analytical uncertainty, not to uncertainty introduced by the $U^{k'}_{37}$ — temperature calibration, therefore the SST variations discussed in the text are meaningful. Alkenone-based SST reconstructions have become a routine tool in paleotemperature studies. Like all paleoceanographic proxies the method has some limitations mostly linked to ecological features of the producer organisms (seasonality, depth of maximum production etc., see Herbert (2003) for a thorough review). In most cases, the time of maximum abundance of *E. huxleyi* and/or *G. oceanica*, and the maximum flux of alkenones into sediment traps, coincides with the dominant period for phytoplankton blooming. Furthermore, temperatures during the season of maximal alkenone production generally come close to mean annual SST (Herbert, 2003). For the Mediterranean Sea (and particularly the eastern basin) limited present day data are available. A previous study has suggested that $U^{k'}_{37}$ temperature reconstructions agree well with mixed layer winter-spring SST averages (Emeis et al., 2000). In addition a sediment trap study in the western Mediterranean has shown maximum alkenone production in spring while maximum production depth is 30–50 m (Ternois et al., 1996).

For the chlorin analysis, 36 freeze-dried sediments were extracted with DCM:MeOH (3:1, v/v) using MARS microwave accelerated reaction system (Kornilova and Rosell-Mele, 2003). Acetone solutions have been analysed by UV absorbance employing an off-column HPLC system with on-line PDA detector. Chlorin concentration has been calculated using *phyropheophorbide a* standard.

Calculations of accumulation rates (AR) (μg cm^{-2} kyr^{-1}) for biomarkers and chlorins have been calculated according to the equation:

$$\mathrm{AR}\left(\mu g\,cm^{-2}kyr^{-1}\right) = \text{absolute biomarker amount}\left(\mu g\,g^{-1}\right) \times \text{sediment accumulation rate}\left(cm\,kyr^{-1}\right) \times \text{dry bulk density}\left(g\,cm^{-3}\right)/1000.$$

Dry bulk densities equal 1.45 g cm^{-3} for the interval above S1, 1.375 g cm^{-3} for S1 interval and 1.55 g cm^{-3} for the sediments below S1 (Roussakis et al., 2004).

5. Results

5.1. $CaCO_3$, TOC and Ba/Al ratio

Calcium carbonate ($CaCO_3$) concentrations in core NS-14 are higher than 26% from 12.6 ka BP until the onset of sapropel S1 deposition, which occurs at 10 ka BP (Fig. 3A). $CaCO_3$ decreases and remains generally lower than 24% throughout the sapropel layer, with a prominent reduction to values as low as 16% at 8.4 ka BP. From the sapropel termination, at 6.4 ka BP, to 4.3 ka BP, $CaCO_3$ increase again to an average value of 24%. Overall, this pattern agrees with the $CaCO_3$ (Fig. 3A) profiles in several other S1 sapropel layers (e.g. Mercone et al., 2001; Slomp et al., 2004), in which the organic-rich intervals display lower $CaCO_3$ contents than surrounding non-sapropel sediments.

Fig. 3B shows typical non-sapropel TOC values (0.2 to 0.4%) between 13 and 10 ka BP (Fig. 3B). Concentrations increase within the S1a and S1b layers, which average values are of 0.9% and 0.7%, respectively. In the interruption, TOC decreases to 0.55%, but never returns to the very low pre-sapropel levels, similarly to what has been noted in previous studies (Mercone et al., 2001; Gogou et al., 2007). Overall, the highest TOC values (1.3%) are observed in the S1a interval.

The Ba/Al ratios (Fig. 3C) are generally low. This might indicate condition of low productivity (McManus et al., 1998) and/or increased terrigenous input. Taking into account that barium accumulation does not correlate with primary productivity in shallow depositional

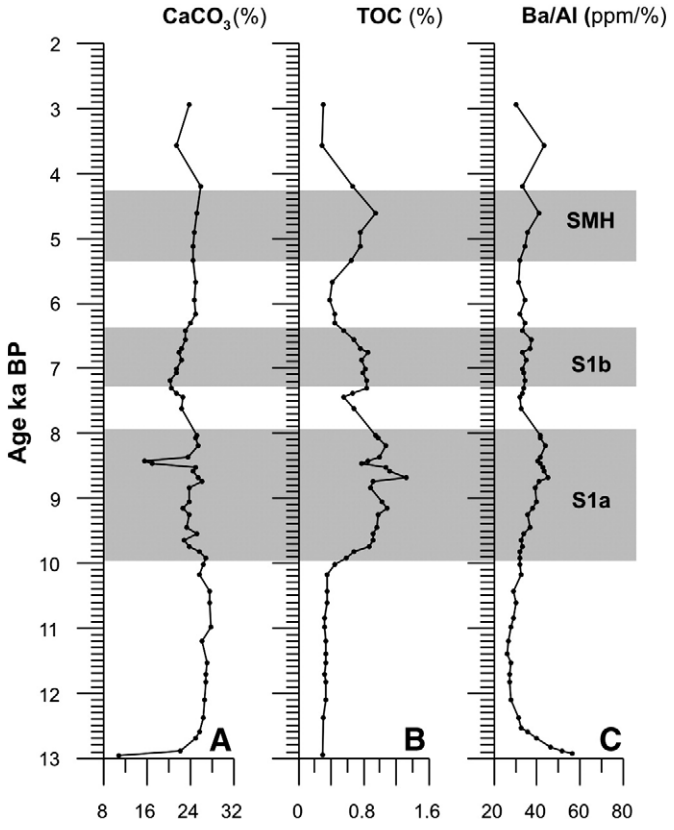

Fig. 3. $CaCO_3$ (%), TOC (%) and Ba/Al (ppm/%). S1a, S1b and SMH sapropelic layers are indicated in dark gray.

environments (Von Breymann et al., 1992), our data are in good correlation with results presented by De Lange et al. (2008) of low Ba/Al ratios and TOC concentrations at shallow depths in the Aegean during S1 deposition. Relatively increased TOC and Ba/Al values are noted mainly in the S1a layer and during 5.4–4.3 ka BP (SMH deposition). Finally, Ba/Al is higher between ~13 and 12.5 ka BP (see Section 6.1) and at around 3.6 ka BP, but the latter peaks are not associated with similar peaks in TOC. In particular the peak at ~3.6 ka BP corresponds to a sample taken from Z2 Santorini ash layer, an interval exhibiting high Ba/Al values (Reitz et al. 2006).

5.2. Coccolithophore assemblages

Emilinia huxleyi dominates the coccolithophore assemblages between 13 and 10.6 ka BP with relative abundances greater than 60% (Fig. 4A). Following this interval and until 7.7 ka BP, this taxon oscillates between 40 and 60%, followed by a distinct minimum of ~500 years. From 6.6 ka BP on *E. huxleyi* shows again oscillations around 60% with two distinct minima centred on 6.0 and 4.8 ka BP. *Emiliania huxleyi* Moderately Calcified morphotypes (EHMC; see Fig. 4B), are found almost exclusively between 13 and 10.0 ka BP and from 6.8 ka BP on, with a distinct maximum abundance centred on 3.5 ka BP. *F. profunda* starts to increase in abundance below S1 at 10.6 ka BP, presenting positive shifts at 8.5, ~7.5, 6.0 and 4.8 ka BP. A profound decrease in *F. profunda* is recorded at ~7.2 and between 6.8 and 6.5 ka BP towards the top of S1b interval (Fig. 4C). In addition, *Helicosphaera* spp. (mainly *H. carteri*; Fig. 4D) starts to increase at 10.6 ka BP, peaking in the lower part of S1a between 10.0 and 9.3 ka BP. A second interval with high abundances of *Helicosphaera* spp. occurs during the formation of the SMH layer. *Braarudosphaera bigelowii* increases significantly at 6.5 ka BP in the upper part of S1b; this species persists with low abundances to 4.6 ka BP (Fig. 4E). *Rhabdosphaera* spp. are reduced during S1 interruption (Fig. 4F). The

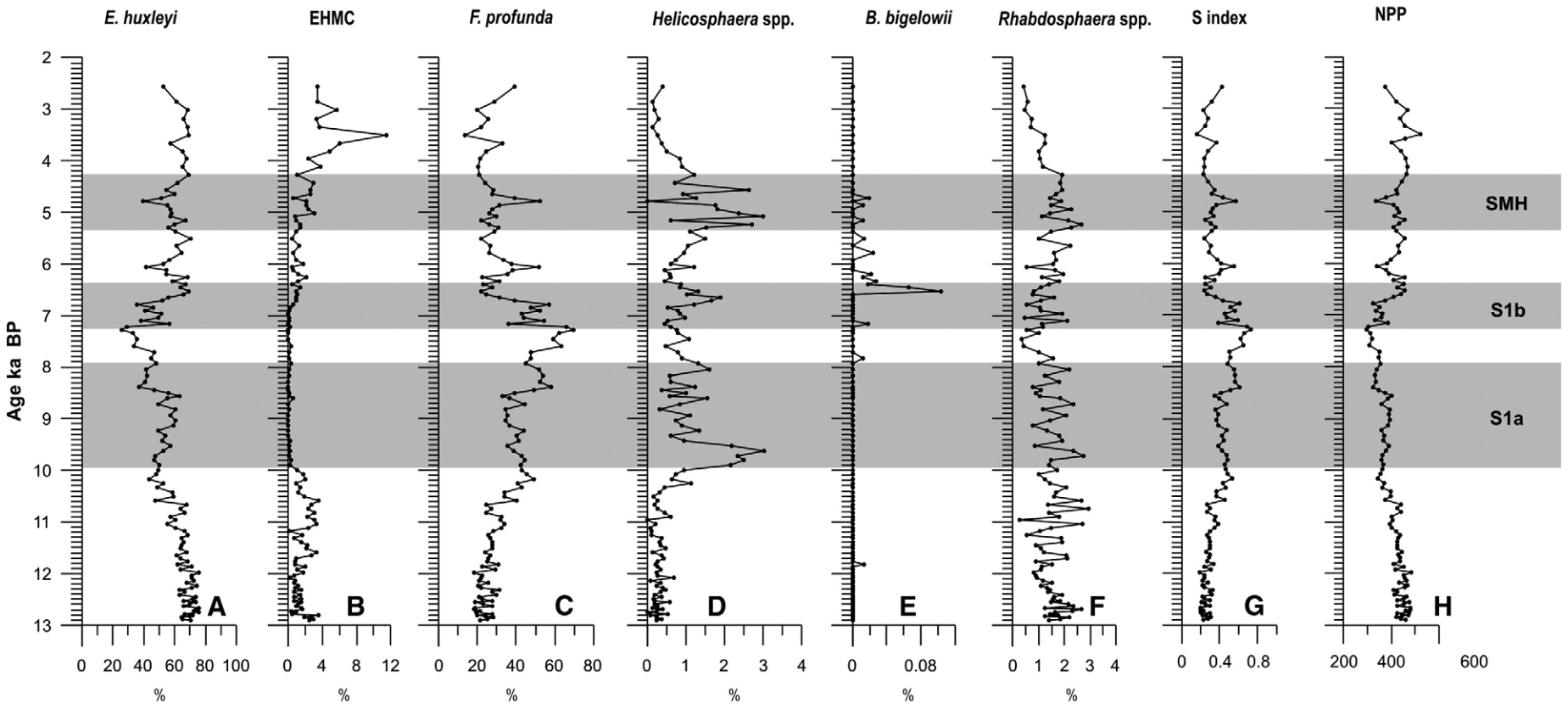

Fig. 4. Relative abundance of coccolithophore species for the core NS-14 expressed in percent.

main positive shifts in the water column stratification, as indicated by the stratification index (S; Fig. 4G), occur at 10.6, 8.5, ~7.5, 6.0 and 4.8 ka BP, reflecting increased coccolithophore (*F. profunda*) productivity in the deeper photic zone. The calculated net primary production (NPP, Fig. 4H) is anticorrelated with *F. profunda* percentages and *S* index, implying shoaling of the nutricline and higher production in the surface layer (Beaufort et al., 1997; Incarbona et al., 2008).

5.3. Pollen records

Deciduous forest elements show their highest abundance between 10.0 and 4.3 ka BP; values are lower outside the sapropel layers S1a, S1b and SMH (Fig. 5A, B). *Cedrus* (Fig. 5C) is present until 3.5 ka BP reflecting the existence of high altitude conifer forests in the circum-eastern Mediterranean area (Combourieu-Nebout, 1998; Mudie et al., 2002). Other conifers (Fig. 5D) appear less abundantly and are mainly represented above ~7.3 ka BP. Mediterranean elements (Fig. 5E) appear almost constantly from 10.0 ka BP on; with short absence intervals during the S1 interruption (around 7.8 ka BP) and above the deposition of S1 (at ~6 kyr cal. BP), also featured by the drop in deciduous *Quercus*. After 4.0 ka BP a rise in the Mediterranean elements is observed. Steppe vegetation elements, such as Compositae, Chenopodiaceae and Poaceae, occur in high numbers before 10.0 ka BP (Fig. 5F–H). The curve of Chenopodiaceae, shows a profound maximum between ~10.7 and 10.0 ka BP (Fig. 5G). It is of particular interest that the expansion of Chenopodiaceae between ~10.7 and 10.0 ka BP (Fig. 5G), a taxon typical for very cold and dry climates in the eastern Mediterranean region (e.g. Rossignol-Strick, 1995), does not reflect in our case the presence of a cold and dry event, but possibly indicates a salt marshy coastal zone in the vicinity (e.g. Geraga et al., 2000).

The semi-desert taxa *Ephedra* and *Artemisia,* although almost continuously present in low numbers in the record, show relatively higher abundances in samples older than ~10.6 ka BP (Fig. 5I, J). The concentration of aquatic palynomorphs is distinctively increased within the sapropel layers (Fig. 5K), tentatively interpreted as representing a strong pulse of continental runoff. The calculated humidity index (H; Fig. 5L) reflects repeated wet phases corresponding to S1a, S1b, SMH depositional intervals. After 4.3 ka BP the progressive increase in Mediterranean elements, Poaceae and *Artemisia* has been attributed to the drier, close to modern, climatic conditions (Mudie et al. 2002) and finally corresponds to the human alternated vegetation described as Beyşehir Occupation Phase of southwest Turkey (Bottema and Woldring, 1990).

5.4. Benthic foraminifera

The foraminiferal density is generally low in our core (Fig. 6A). The species *Hoeglundina elegans*, *Melonis barleeanum*, *Uvigerina mediterranea*, *Gyroidina altiformis* and *Bulimina marginata* show abundance peak between 11.0 and 10.0 ka BP, just below the base of S1 (Fig. 6I–M). At this point the faunal assemblage declines, coinciding with the increase in abundance of the species *Bolivina alata*, *Globobulimina affinis*, *Chilostomella mediterranensis*, *Valvulineria bradyii* and *Bulimina costata* throughout the S1 depositional interval (Fig. 6B–F). The rapid re-appearance and dominance of *Planulina ariminensis*, *Bulimina inflata*, *M. barleeanum*, *U. mediterranea* and *G. altiformis* at ~6.5 ka BP, marks the end of S1 (Fig. 6G–H, J–L). However *G.affinis* and *C. mediterranensis* present another remarkable increase from 5.4 to 4.3 ka BP within the SMH layer (Fig. 6C–D), associated with high percentages of *V. bradyii*, *B. alata* and *B. costata.* Above this level and up to the top of the core *M. barleeanum*, *U. mediterranea*, *G. altiformis, B. inflata, B. marginata* and *P. ariminensis* become once more the most abundant species in the assemblages.

5.5. Organic biomarkers

Marine sterols are major constituents of several marine phytoplankton groups such as prymnesiophytes, diatoms and dinoflagellates (Volkman et al., 1999; Menzel et al., 2003; Gogou et al., 2007). Long chain C_{37} and C_{38} alkenones are biosynthesised by some haptophyte algae (e.g. Marlowe et al., 1984). Outside the sapropel layers both marine sterols and alkenones have low Accumulation Rates (ARs) (mean ARs are 1.40 μg cm^{-2} kyr^{-1} and 1.60 μg cm^{-2} kyr^{-1} respectively; Fig. 7B, C), which may be related to low productivity in surface waters and/or reduced preservation in well-oxygenated bottom waters (Gogou et al., 2007). Elevated marine sterol concentrations are observed mainly within the sapropel sub-layer S1a (average ARs are 3.6 μg cm^{-2} kyr^{-1}) and are typical of higher productivity and/or better preservation of the organic matter (Bouloubassi et al., 1998; Menzel et al., 2003; Gogou et al., 2007). During the same interval loliolide and isololiolide ARs, compounds that are diagenetic products of carotenoids under reducing conditions in marine sediments (Klok et al., 1984; Repeta, 1989), express their maximum values (average ARs 4.2 μg cm^{-2} kyr^{-1}; Fig. 7D). The chlorophyll *a* degradation products, collectively named chlorins, are directly derived from phytoplankton activity and have often been used to reconstruct past primary productivity (e.g. Harris et al., 1996). Chlorin concentration in our sequence follows the general pattern of enhanced ARs at higher TOC concentrations (Fig. 7E); values are very low outside organic-rich layers, but reflect higher total primary productivity and favourable preservation conditions especially within the sapropelic interval S1a (average ARs 36.3 μg cm^{-2} $kyr^{-}1$) and to a lesser degree during S1b and SMH (average ARs 25.6 and 28.8 μg cm^{-2} $kyr^{-}1$ respectively). Ter-alkanols exhibit higher ARs within the sapropelic layer S1a in comparison to S1b and SMH (up to 14.2, 10.4 and 6.2 μg cm^{-2} kyr^{-1} respectively; Fig. 7F) and suggest increased river runoff (Aksu et al., 1995; Bouloubassi et al., 1998; Menzel et al., 2003; Gogou et al., 2007).

5.6. Alkenone-based Sea Surface Temperatures (SSTs)

The Sea Surface Temperature (SST; Fig. 8) estimated from the alkenone unsaturation index Uk'_{37} reveals quasi-uniform temperatures (17.0–18.7 °C) in the interval from ~13 to 10.5 ka BP. A temperature increase of 3.2 °C at ~9.9 ka BP predates a decrease down to 17.4 °C at 9.7 ka BP, at the lower part of S1a. Within the sapropel layer S1a the temperatures increase gradually and have an average value of 19.5 °C (Fig. 8). A drop in SST of about 1.6 °C occurs at ~8.5 ka BP. The S1 interruption is featured by temperatures of about 21 °C, whereas there is a low amplitude fluctuation of SST values within the S1b layer, although average values are still centred on 21 °C. SSTs fluctuate between 5.4 and 4.3 ka BP during the SMH deposition, with an average value of 22 °C and a prominent positive excursion to 24.9 °C at ~4.9 ka BP. Temperature decreases down to 18.5 °C at ~3 ka BP similar to the values calculated in the North Aegean (Gogou et al., 2007).

6. Discussion

6.1. The Late Glacial to early Holocene interval

Emiliania huxleyi Moderately Calcified (EHMC) morphotypes, which are restricted to cool Holocene intervals (Crudeli et al., 2004), feature the present day Aegean during winter/spring (Dimiza et al., 2008) associated with temperatures between 16 and 19.5 °C (Poulos et al., 1997). In comparison, Uk'_{37}SST displays similar values between ~13 and 10.6 ka BP (Fig. 8) and together with the high EHMC abundances (Fig. 4B) point to generally cool surface waters during the transition to the Holocene.

On land, the occurrence of semi-desert taxa *Ephedra* and *Artemisia* between ~13 and 10.6 ka BP (Fig. 5I, J) reflects drier climate. Yet, the coexistence of deciduous *Quercus* and conifers imply sufficient

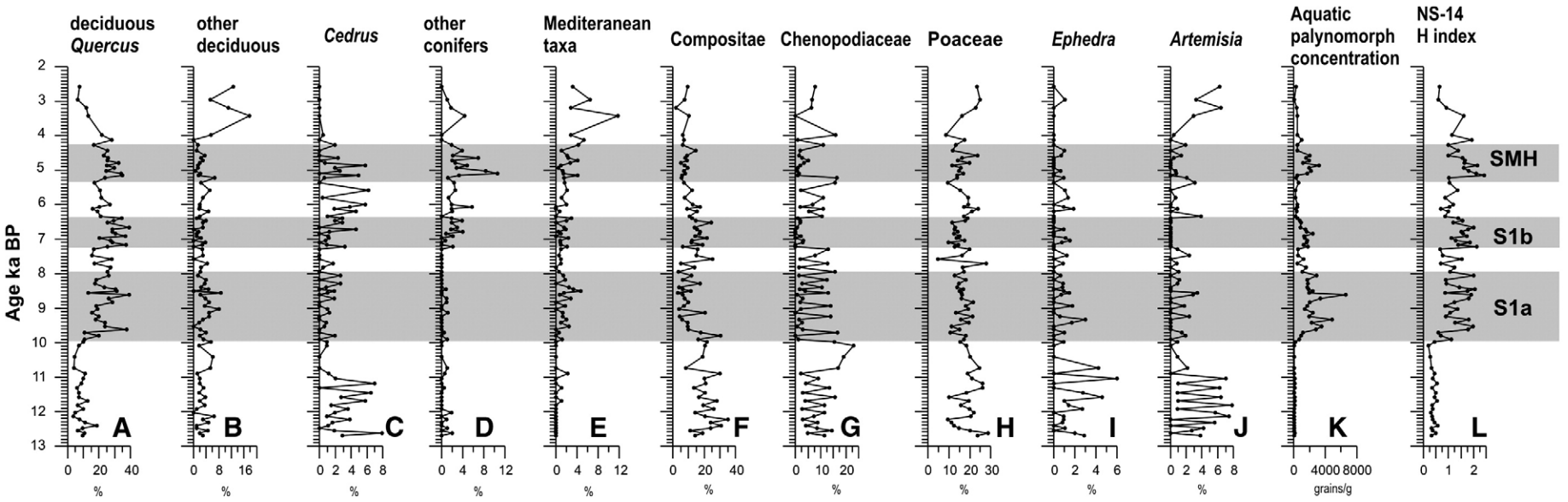

Fig. 5. Abundance curves of the most indicative pollen groups in core NS-14. Conifers include *Abies* and *Picea*, deciduous taxa include *Acer, Carpinus, Corylus, Juglans, Alnus* and *Ulmus* and Mediterranean taxa include *Olea* and *Pistacea.*

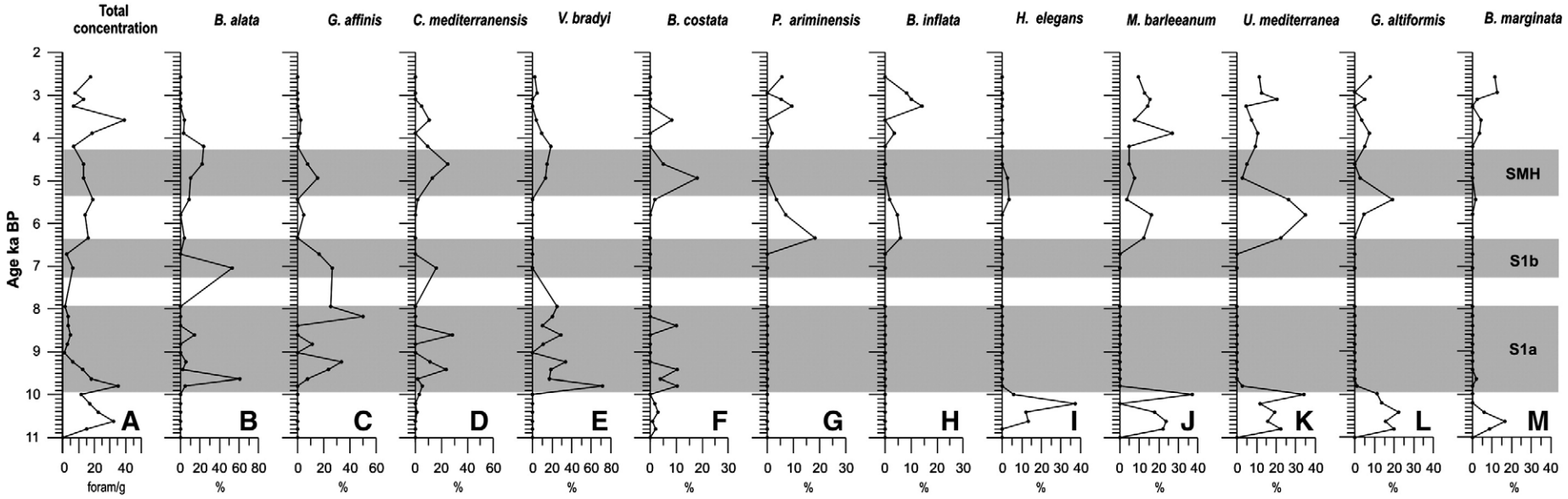

Fig. 6. Abundance curves of the most indicative benthic foraminiferal species in core NS-14.

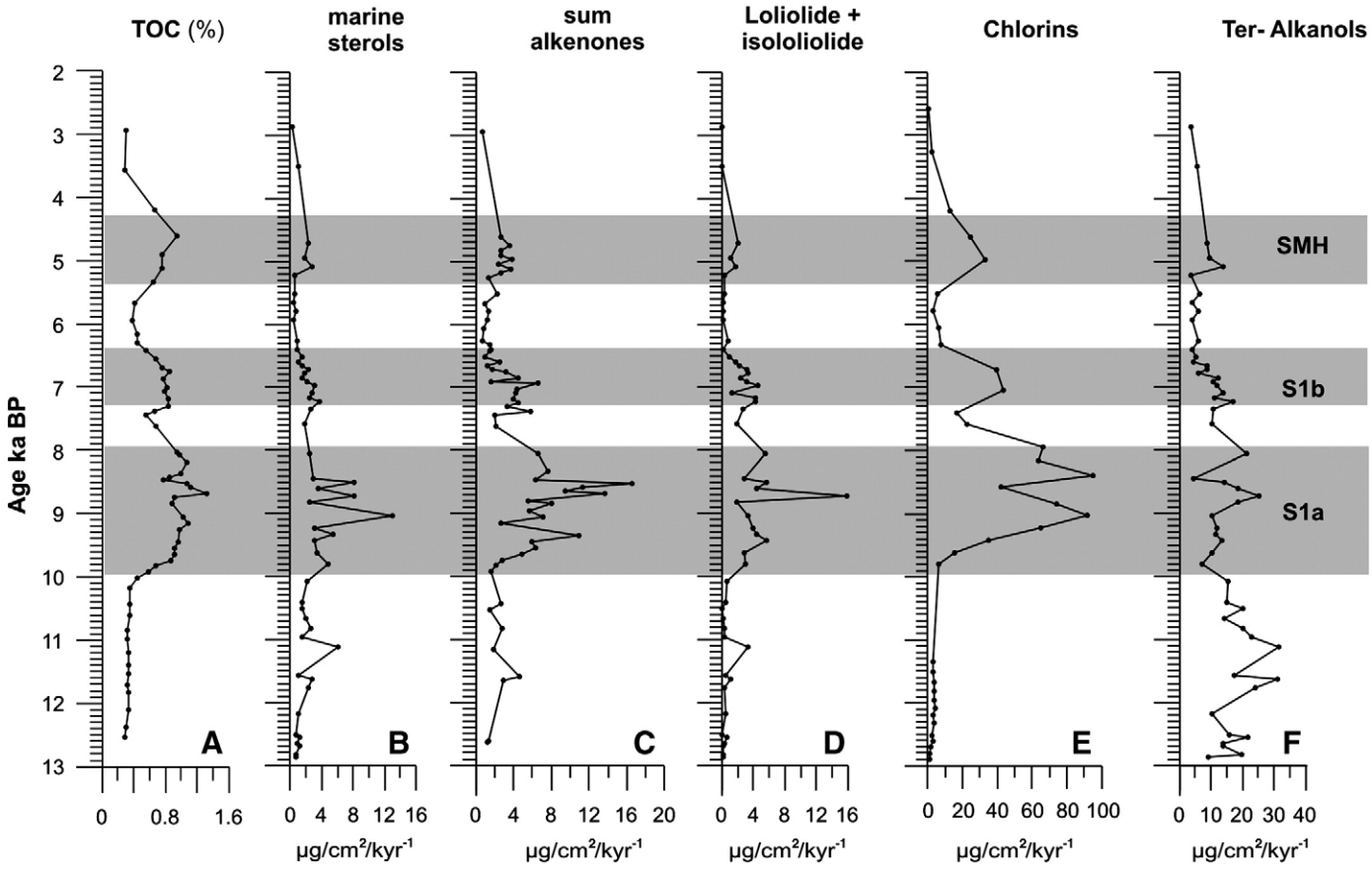

Fig. 7. Accumulation rates of the investigated organic biomarkers.

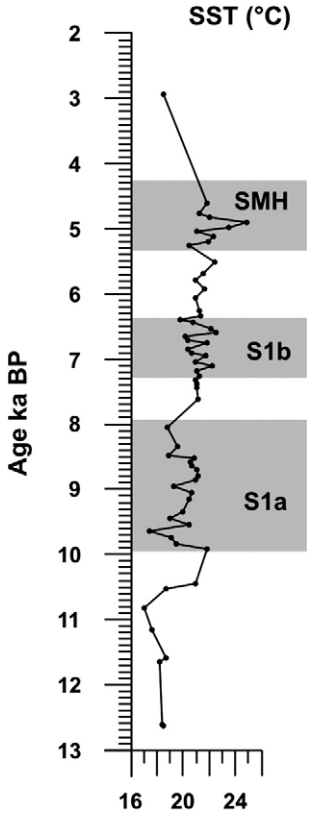

Fig. 8. $U^{k'}_{37}$ SST values in NS-14.

precipitation, also reflected by the high ARs of Ter-alkanols (Fig. 7F). This should have allowed the development of forest vegetation in favourable areas. The sporadic presence of Mediterranean elements after 11.8 ka BP marks a rise in winter temperatures.

The high Ba/Al values at ~13–12.5 ka BP (Fig. 3C) could be associated with the decreased carbonate concentrations at the same levels (Fig. 3A). In particular, decreased carbonate production and increased total marine productivity suggest a switch to the dominance of opportunistic species, such as diatoms (Van Os et al., 1994). The low biomarker and TOC content (Fig. 7) until 12.5 ka BP compared to a more variable Ba/Al profile with relatively high values, is here interpreted to reflect intervals of intensified degradation processes under oxic conditions, which likely mask the original high primary production signal (Aksu et al., 1999; Sinninghe Damsté et al., 2002). Taken together, these evidence suggest that during the Late Glacial cold and dry climate conditions in the (south-eastern) Aegean co-existed with well ventilated intermediate waters and, in turn, reduced preservation of organic matter. This agrees with a recently proposed scenario of intensified ventilation processes in the Aegean water column during episodes of harsh climate (Casford et al., 2003).

6.2. The deposition of S1 in the south-eastern margin of the Aegean Sea

In the shallow south-eastern Aegean NS-14 core the onset of the visual S1 at 10.0 ka BP, coincides with the abundance increase of the deep and intermediate-deep benthic foraminifera infaunal taxa *C. mediterranensis*, *G. affinis* (Fig. 6C, D), and the oxygen deficiency indicators *V. bradyii*, *B. alata* and *B. costata* (Rohling et al., 1997; Kuhnt et al., 2007; Abu-Zied et al., 2008). This age fits well with the ages reported from other Aegean records (e.g. Perissoratis and Piper, 1992; Aksu et al., 1995; Geraga et al., 2000; Casford et al., 2002; Roussakis et al., 2004; Gogou et al., 2007; De Lange et al., 2008). The duration

(10.0 to 6.4 ka BP) is comparable to the mean S1 duration (9.8 to 6.5 ka BP) estimated in the Aegean Sea cores in which chronologies have been accurately tested against Greenland ice-core chronologies (Rohling et al., 2002b; Casford et al., 2007). Minor age discrepancies concerning the initiation of S1 in the core NS-14 reflect the local conditions of marine circulation, depositional depth and the amount of the organic material that reaches the sea floor. The upper age limit may also differ due to post depositional processes (De Lange et al., 1989; Higgs et al., 1994; Thomson et al., 1999), however such result cannot be evaluated from our low TOC and Ba/Al records.

Before the onset of S1 deposition (between 10.6 and 10.0 ka BP), the gradual increase of *Helicosphaera* spp. (see Fig. 4D), a coccolithophore group that is associated with lowering in salinity (Flores et al., 1997; Colmenero-Hidalgo et al., 2004), possibly indicates higher fresh water input in the core site. In addition our records indicate a relevant increasing trend featuring the nutricline depth proxy *F. profunda* (Fig. 4C) and the stratification *S* index (Fig. 4G), which support the establishment of stratified conditions and the onset of nutrient-rich environment in the deep photic zone prior to S1 depositional interval. Further, at the sediment surface the increasing abundance of the more mesotrophic–oligotrophic benthic foraminifera (Fontanier et al., 2002) *H. elegans*, *M. barleeanum*, *U. mediterranea* and *G. altiformis* (Fig. 6I–L), reflects a general impoverishment of the sea floor, as a result of reduction of deep water ventilation, similarly to what has already been observed in other shallower and deeper locations in the Aegean Sea before the onset of S1 (e.g. Kuhnt et al., 2007; Abu-Zied et al., 2008).

The pollen record across the S1a sapropelic layer, displays an increase of Mediterranean taxa (Fig. 5E) suggesting a positive trend towards warmer conditions, whereas Uk'_{37} temperatures have an average value of 19.5 °C (Fig. 8). A decline in surface water salinity is assumed between 10.0 and 8.5 ka BP by the increase of *Helicosphaera* spp. (Fig. 4D), followed by a concomitant increase of the stratification *S* index mainly above 8.5 ka BP. The fresh water input in the south-eastern margin of the Aegean Sea is also corroborated by the increased aquatic palynomorph concentrations (Fig. 5K). The positive shifts of the humidity *H* index at our site (Fig. 5L), are attributed to an increase in regional precipitation. This interpretation is in agreement with what has been found by Kotthoff et al. (2008) in a northern Aegean record. The increased ARs of Ter-alkanols (Fig. 7F) further suggest the high supply of terrigenous material, ascribed to increased land runoff.

The S1 interruption (7.9–7.3 ka BP) in south-eastern Aegean proves to be an interval characterised by alkenone surface temperatures that are stable around 21 °C (Fig. 8). Similar results have been recorded in the Southern Adriatic Sea by Giunta et al. (2003) and Sangiorgi et al. (2003) who estimated an U^{k}_{37} SST warming of about 1.5 °C during S1 interruption. Our data from NS-14 south-eastern Aegean core show the absence of Mediterranean elements for a short interval around 7.8 ka BP representing a short period of climatic deterioration (Rossignol-Strick, 1995). A drop in precipitation during S1 interruption is featured by the decline in aquatic palynomorphs (Fig. 5K) and *H* index (Fig. 5L). In addition, a slight break of stratification (*S* index, Fig. 4G), coupled to the concomitant decrease of oligotrophic surface waters indicator *Rhabdosphaera* spp. (Winter et al., 1994), also testifies reinvigoration of deep convective processes (Rohling et al., 1997; De Rijk et al., 1999; Mercone et al., 2001; Casford et al., 2003). *S* index is once more increasing before the onset of S1b. Therefore, it seems more likely that S1 interruption in the south-eastern Aegean Sea does not reflect a very cold and dry spell as evidenced in higher latitude locations (e.g. Rohling et al., 1997; De Rijk et al., 1999), but it may rather correlate with a weakening in the African monsoon intensity (e.g. Rohling et al., 2004).

The SST coolings as reflected by the Uk'_{37} variability mainly within S1b layer (Fig. 8), may be linked to outbursts of cold northerly air masses from eastern European and Siberian sources (e.g. Rohling et al., 2002b; Geraga et al., 2005; Gogou et al., 2007; Marino, 2008). Related to that, the increase of conifers above 7.0 ka BP (Fig. 5D), mainly attributed to *Picea*, is indicative of north wind outbursts (Mudie et al., 2002). Sea surface cooling during these intervals of climatic deterioration was, however, not intense enough to promote vigorous convective processes and consequently interrupt sapropel deposition. Yet, the enhanced surface buoyancy loss coupled to these events was such to disrupt the surface to intermediate water stratification (see variations of stratification *S* index; Fig. 4G). In particular, the profound decrease of *F. profunda* at the upper part of S1 (Fig. 4C) confirms the decline of Deep Chlorophyll Maximum (DCM) throughout the Eastern Mediterranean at ~6.5 ka BP (e.g. Giunta et al., 2003; Principato et al., 2003, 2006). More specifically, the negative shift in *S* index and the peak of NPP at ~6.5 ka BP (Fig. 4G, H) evidences lowering of stratification, most probably associated with fresh water input that is marked now by the increase of *B. bigelowii* (Fig. 4E), a hyposaline and relatively eutrophic nannofossil indicator (Boalch, 1987; Negri and Giunta, 2001). A similar increase of this species has also been recorded at the same time interval in the eastern Ionian (Negri and Giunta, 2001), interpreted as stratification increase, and from the area west-southwest of Crete (Principato et al., 2003) being related to runoff conditions during a wet and cold period. Because our organic biomarker data at this point (low input of Ter-alkanols; Fig. 7F) do not support freshening of surface waters as a result of riverine input, the second hypothesis which suggests cooling before the end of S1 sapropelic conditions seems more plausible. The concomitant increase of the shallow and intermediate infaunal *M. barleeanum* and *U. mediterranea* (Fig. 6J, K) along with the simultaneous decline of the dysoxic deep infaunal species *G. affinis* and *C. mediterranensis* (Fig. 6C, D) marks the re-oxygenation of bottom waters at this time interval, illustrating a progressive increase of the trophic level in the water column. The associated drop in Mediterranean elements and in deciduous *Quercus* (Fig. 5A) further records the climatic deterioration that features the end of S1.

Our records indicate dysoxic bottom-water conditions during the deposition of S1 at the south-eastern edge of the Aegean Sea. This observation is supported by the maxima of loliolide and isololiolide ARs, restricted only within the S1a interval (Fig. 7D). In addition, isorenieratene, a pigment derived from anoxygenic photosynthetic sulphur bacteria found in sapropels (e.g. Menzel et al., 2002), is absent in all samples, comparable to similar findings in the N. Aegean during S1 (Gogou et al., 2007) or in south-eastern Aegean during more extreme sapropel events (Marino et al., 2007). The absence of isorenieratene in NS-14 during S1 implies that intermediate waters were – at least – occasionally ventilated during the deposition of S1, which is a conclusion also claimed in previous studies (Aksu et al., 1995; Mercone et al., 2001; Casford et al., 2002, 2003; Kuhnt et al., 2007; Abu-Zied et al., 2008; Marino, 2008). Furthermore the presence of dysoxic benthic foraminiferal indicators that continue throughout sapropel S1 in core NS-14, indicates that long term anoxia never developed in this site in accordance to what has been observed in other shallow Aegean cores (e.g. core SL-31, 430 m depth; Abu-Zied et al., 2008). The mean TOC concentration in our S1 layers is low, also affected by dilution due to high sedimentation rates (Mercone et al., 2000) and by the prevailing weakened anti-estuarine circulation (e.g. Rohling and Gieskes, 1989; Rohling, 1994; Stratford et al., 2000).

The warm and humid climate prevailing during the formation of S1 and the relevant water column stratification (Figs. 4G, 5L) are expected to enhance production and preservation of organic matter (e.g. Rohling and Gieskes, 1989). However, our micropaleontological and geochemical evidence cannot prove unequivocally that marine productivity actually rose during S1 times at the south-eastern margin of the Aegean Sea. The higher TOC, marine sterol and chlorin values and the increase of both coccolithophore productivity proxies *F. profunda* (Molfino and MacIntyre, 1990) and *Helicosphaera* spp. (Ziveri et al., 2004; Crudeli et al., 2006), together with the inversely related NPP, do outline a productive deeper photic zone (see

Figs 3–7). However, the climate instability and the relevant absence of anoxia in the shallow western Kos Basin caused weak preservation of the organic matter. The values are much higher within S1a confirming the findings of Gogou et al. (2007) in the North Aegean that marine productivity and/or more favourable conditions for organic matter preservation were significantly higher before the S1 interruption than during the formation of S1b layer.

6.3. Evidence for on-going humidity in the mid Holocene: deposition of the sapropel-like layer SMH between 5.4 and 4.3 ka BP

A series of SST fluctuations are detected in our data set between 5.4 and 4.3 ka BP (Fig. 8), with a sharp positive shift to 24.9 °C at ~4.8 ka BP. During the same interval we recorded high numbers of the coccolithophore *Helicosphaera* spp. (Fig. 4D) which is indicative of salinity decrease, high aquatic palynomorph concentrations (Fig. 5K), as well as higher accumulations of Ter-alkanols (Fig. 7F) which are indicative of continental (river) runoff. Taken together, these observations point to an increased supply of freshwater to the NS-14 core site. At the same time, pollen evidence suggests the expansion of deciduous forest elements and increased pollen-induced humidity *H* index (Fig. 5L). As a result, stratified conditions in the water column and increased productivity in the deep photic zone are evidenced at ~4.8 ka BP by the positive trend recorded in the *F. profunda* abundance and the increased values of the stratification *S* index (Fig. 4C, G). TOC (~1%), Ba/Al, marine sterols and chlorin patterns are similar to those recorded within the sapropel layer S1b (see Figs 3, 7) possibly reflecting limited preservation due to the shallow depositional depth and the climatic instability. The slight increase of the organic biomarker loliolide (Fig. 7D) and the concomitant abundance peak of such deep infaunal low-oxygen tolerant foraminifers as *G. affinis* and *C. mediterranensis* (Fig. 6C, D), support the establishment of at least dysoxic conditions at depth during the 5.4–4.3 ka BP time interval.

Several observations document humid conditions in the Near and Middle East and the Arabian Sea during the mid Holocene. These refer to the onset of moist conditions between 5.2 and 4.2 ka BP recorded from lake sediments in south-eastern Arabia (Parker et al., 2006), the second aridification step reported from NE Africa between 6 and 3.8 kyr BP (Jung et al., 2004), and the humid phase recorded during ~5.2–4.4 ka BP in the Dead Sea (Migowski et al., 2006). The "palaeo annual rainfall" calculated from the speleothem paleoclimate record from the Soreq Cave in Israel (Bar-Matthews et al., 2003) also displays a small peak in rainfall at about 4.7 ka. Robinson et al. (2006) proposed a "mid Holocene wet event" at ~5 kyr BP while reviewing several terrestrial data sets. Additional evidence from the Marathon coastal plain in E. Greece (Pavlopoulos et al., 2006) implies warm, strongly seasonal climate during 5.8 and 3.5 ka BP. Furthermore, recent research based on the distribution of the terrigenous fraction in marine sediments (Hamann et al., 2008) has shown a humidity maximum at 5 ka BP coincident with a regional wet phase in the Levantine Sea.

Our findings in the core NS-14 for sustained warm and humid conditions after 5 ka BP during the mid Holocene, probably associated with enhanced precipitation and influx of low-salinity waters from the Black Sea (Sperling et al., 2003), support the establishment of stratified conditions at least in semi-enclosed basins. We propose that this process triggered suboxic conditions for a period of ~1000 years and gave rise to the deposition of a regional sapropel-like layer, the Sapropel Mid Holocene layer (SMH) between 5.4 and 4.3 ka BP (5–4 kyr uncal. BP), traced in our case in the shallow but partially closed western Kos Basin. Interestingly, a sapropelic layer (Upper sapropel layer; Tolun et al., 2002) of similar age (4.75–3.2 kyr uncal. BP) has been recorded in the Marmara Sea, well above the equivalent of sapropel S1 in this basin, associated with the establishment of the dual flow regime between the Black Sea and the eastern Mediterranean (Çatağay et al., 2000). The deposition of the organic matter-rich layer SMH was terminated abruptly at 4.3 ka BP, coinciding with a significant Northern Hemisphere rapid climate cooling (Mayewski et al., 2004; Booth et al., 2005; Migowski et al., 2006) and a concomitant reduction of Black Sea surface water flow (e.g. Sperling et al., 2003). Additionally, it is in good agreement with the termination of the African Humid Period at 3.8 ka BP, off the western coast of Africa (Jung et al., 2004). This cooling event is expressed at low-latitudes as a mega-drought event that caused the collapse of Akkadian Empire in the Middle East by the displacement of the Mediterranean westerlies and the Indian monsoon (Weiss et al., 1993; Cullen et al., 2000).

The presence of the sapropel-like layer SMH has not been recorded in other cores (e.g. Aksu et al., 1995, 1999; Mercone et al., 2000; Rohling et al., 2002b; Kotthoff et al., 2008) in the Aegean Sea, although sedimentation rates are comparable to our record. Our alkenone SST data reveal significant cool/warm fluctuations throughout SMH. These fluctuations suggest short-term intervals of climate instability and possibly intermittent periods of water column ventilation, which would have impeded the organic-rich deposition in other records. However we cannot exclude the effect of local oceanographic and productivity conditions (Stratford et al., 2000; Casford et al., 2003) on sapropel deposition. In conjunction with statements in Cane et al. (2002) and Rohling et al. (2002a) suggesting that S1 was relatively short lived and may have not been strong enough to re-establish after the cold outbreak around 6 ka BP, our finding of the SMH layer could represent evidence of on-going, albeit weak, mid Holocene African monsoon forcing, only expressed in this sensitive locality at the south-eastern edge of the Aegean Sea.

7. Conclusions

A multi-proxy study of south-eastern Aegean core NS-14 provides a portrayal of the climate and oceanographic changes in the region over the last ~13 ka BP. Our micropaleontological (coccolithophores, benthic foraminifera), palynological (pollen), and geochemical (TOC, CaCO3, Ba/Al, marine sterols, chlorins, alkenone-based SST) results provide a detailed record of primary production and organic matter preservation during sapropel S1 deposition at intermediate depths and reveal the influence of the northern hemisphere climate variability on the SE Aegean deposits. In addition, the studied marine record displays significant information concerning the climatic and oceanographic conditions in the Aegean during the mid-Late Holocene time interval.

The major conclusions of this study are summarized as follows:

(1) The deposition of sapropel S1 at intermediate depths in the south-eastern Aegean Sea took place between 10.0 and 6.4 ka BP, with an interruption between 7.9 and 7.3 ka BP.
(2) The presented results state that freshwater input during ~10.6–10.0 ka BP has preceded the deposition of S1 in the SE Aegean Sea margin. Further decrease in surface water salinity is evidenced between 10.0 and 8.5 ka BP at the lower part of S1a.
(3) The lower part of S1a is featured by warmer (~19.5 °C) and more productive surface waters associated with dysoxic bottom conditions. A series of cooling events may be linked to outbursts of cold northerly air masses and relevant pulses in the deep water ventilation that caused the S1 interruption and culminated during the deposition of S1b, with the decline of DCM at ~6.5 ka BP.
(4) Our analysis confirms the absence of complete anoxia during the S1 times in the shallow south-eastern Aegean margin. This is due to the prevailing anti-estuarine circulation but it is also strongly linked to the recorded climate instability. Both factors are possibly responsible for the weak preservation of the organic matter in the sapropel layers, although it seems that conditions

favouring higher marine productivity and/or organic matter preservation were taking place mainly during the S1a interval.

(5) NS-14 record provides evidence for a distinct mid Holocene warm (up to ~25 °C) and wet phase associated with the deposition of the sapropel-like layer SMH (Sapropel Mid Holocene), between 5.4 and 4.3 ka BP. This finding at the south-eastern margin of the Aegean documents the humid conditions already evidenced in the Levantine Sea (sedimentological evidence of humidity maximum at 5 kyr BP), the Near East (peak in rainfall at about 4.7 ka in the Soreq Cave speleothem record) and Middle East (humid phase recorded during ~5.2–4.4 ka BP in the Dead Sea) and the Arabian Sea (moist conditions between 5.2 and 4.2 ka BP recorded from lake sediments) during the mid Holocene. SMH is featured by significant SST fluctuations throughout its deposition. Its end is associated with the 4.2 ka BP Northern Hemisphere mega drought event that caused the collapse of Akkadian Empire in the Middle East.

Acknowledgements

This work has been made possible thanks to the financial support provided by the Pythagoras I project (EU and Greek Ministry of Education, EPEAEK II) and the partial support from the European Science Foundation (ESF) under the EUROCORES Programme EuroCLIMATE, through contract No. ERAS-CT-2003-980409 of the European Commission, DG Research, FP6 and PENED project 03669 of the European Union and the General Secretariat for Research and Technology, Greek Ministry of Development. Critical comments by C. Fontanier, an anonymous reviewer and the journal editor G. De Lange have proved essential in improving the manuscript.

References

Abu-Zied, R.H., Rohling, E., Jorissen, F.J., Fontanier, C., Casford, J.S.L., Cooke, S., 2008. Benthic foraminiferal response to changes in bottom-water oxygenation and organic carbon flux in the eastern Mediterranean during LGM to Recent times. Mar. Micropaleontol. 67, 46–68.

Aksu, A.E., Abrajano, T., Mudie, P.J., Yasar, D., 1999. Organic geochemical and palynological evidence for terrigenous origin of the organic matter in Aegean Sea sapropel S1. Mar. Geol. 153, 303–318.

Aksu, A.E., Yaşar, D., Mudie, P.J., Gillespie, H., 1995. Late Glacial–Holocene paleoclimatic and paleoceanographic evolution of the Aegean Sea: micropaleontological and stable isotopic evidence. Mar. Micropaleontol. 25, 1–28.

Bar-Matthews, M., Ayalon, A., Gilmour, M., Hawkesworth, C.J., 2003. Sea-land oxygen isotopic relationships from planktonic foraminifera and speleothems in the Eastern Mediterranean region and their implication for paleorainfall during interglacial intervals. Geochim. Cosmochim. Acta 67, 3181–3199.

Beaufort, L., De Garidel-Thoron, T., Mix, A.C., Pisias, N.G., 2001. ENSO-like forcing on oceanic primary production during the late Pleistocene. Science 293 (5539), 2440–2444.

Beaufort, L., Lancelot, Y., Camberlin, P., Cayre, O., Vincent, E., Bassinot, F., Labeyrie, L., 1997. Insolation cycles as a major control of equatorial Indian Ocean primary production. Science 278 (5342), 1451–1454.

Boalch, G.T., 1987. Recent blooms in the Western English Channel. Rapport et Proce©s-verbaux des Rëunions. Conseil. International pour l'Exploration de la Mer, vol. 187, pp. 94–97.

Booth, R.K., Jackson, S.T., Forman, S.L., Kutzbach, J.E., Bettis, E.A., Kreig, J., Wright, D.K., 2005. A severe centennial-scale drought in mid-continental North America 4200 years ago and apparent global linkages. Holocene 15, 321–328.

Bottema, S., 1991. Développement de la végétation et du climat dans le bassin méditerranéen oriental à la fin du Pliocène et pendant l'Holocène. Anthropologie 4, 695–728.

Bottema, S., Woldring, H., 1990. Anthropogenic indicators in the pollen record of the Eastern Mediterranean. In: Bottema, S., Entjes-Nieborg, G., van Zeist, W. (Eds.), Man's Role in the Shaping of the Eastern Mediterranean Landscape. Balkema, Rotterdam, pp. 231–264.

Bouloubassi, I., Guehenneux, G., Rullkötter, J., 1998. Biological marker significance of organic matter origin in sapropels from the Mediterranean ridge, Site 969. In: Robertson, A.H.F., Emeis, K., Richter, C. (Eds.), Proc. Ocean Drilling Program: Scientific Results, vol. 160, pp. 261–270.

Cane, T., Rohling, E.J., Kemp, A.E.S., Cooke, S., Pearce, R.B., 2002. High-resolution stratigraphic framework for Mediterranean sapropel S5: defining temporal relationships between records of Eemian climate variability. Palaeogeogr., Palaeoclimatol., Palaeoecol. 183, 87–101.

Casford, J.S.L., Abu-Zied, R., Rohling, E.J., Cooke, S., Fontanier, Ch., Leng, M., Millard, A., Thomson, J., 2007. A stratigraphically controlled multi-proxy chronostratigraphy for the eastern Mediterranean. Paleoceanography 22, PA4215. doi:10.1029/2007PA001422.

Casford, J.S.L., Rohling, E.J., Abu-Zied, R., Cooke, S., Fontanier, C., Leng, M., Lycousis, V., 2002. Circulation changes and nutrient concentrations in the late Quaternary Aegean Sea: a nonsteady state concept for sapropel formation. Paleoceanography 17 (2), 1024–1034.

Casford, J.S.L., Rohling, E.J., Abu-Zied, R.H., Fontanier, C., Jorissen, F.J., Leng, M.J., Schmiedl, G., Thomson, J., 2003. A dynamic concept for eastern Mediterranean circulation and oxygenation during sapropel formation. Palaeogeogr., Palaeoclimatol., Palaeoecol. 190, 103–119.

Castradori, D., 1993. Calcareous nannofossils and the origin of eastern Mediterranean sapropels. Paleoceanography 8 (4), 459–471.

Çatağay, M.N., Görür, N., Algan, O., Eastoe, C., Tchapalyga, A., Ongan, D., Kuhn, T., Kuşcu, I., 2000. Late Glacial–Holocene palaeoceanography of the Sea of Marmara: timing of connections with the Mediterranean and the Black Seas. Mar. Geol. 167, 191–206.

Colmenero-Hidalgo, E., Flores, J.A., Sierro, F.J., Bárcena, M.Á., Löwemark, L., Schönfeld, J., Grimalt, J.O., 2004. Ocean surface water response to short-term climate changes reealed by coccolithophores from the Gulf of Cadiz (NE Atlantic) and Alboran Sea (W Mediterranean). Palaeogeogr., Palaeoclimatol., Palaeoecol. 205, 317–336.

Combourieu-Nebout, N., Paterne, M., Turon, J.-L., Siani, G., 1998. A high resolution record of the last deglaciation in central Mediterranean Sea: palaeovegetation and palaeohydrological evolution. Quat. Sci. Rev. 17, 303–317.

Cramp, A., O'Sullivan, G., 1999. Neogene sapropels in the Mediterranean: a review. Mar. Geol. 153, 11–28.

Crudeli, D., Young, J.R., Erba, E., de Lange, G.J., Henriksen, K., Kinkel, H., Slomp, C.P., Ziveri, P., 2004. Abnormal carbonate diagenesis in Holocene–late Pleistocene sapropel-associated sediments from the Eastern Mediterranean; evidence from *Emiliania huxleyi* coccolith morphology. Mar. Micropaleontol. 52, 217–240.

Crudeli, D., Young, J.R., Erba, E., Geisen, M., Ziveri, P., de Lange, G.J., Slomp, C.P., 2006. Fossil record of holococcoliths and selected hetero-holococcolith associations from the Mediterranean (Holocene-late Pleistocene): evaluation of carbonate diagenesis and paleoecological–paleogeographic implications. Palaeogeogr., Palaeoclimatol., Palaeoecol. 237, 191–212.

Cullen, H.M., deMenocal, P.B., Hemming, S., Hemming, G., Brown, F.H., Guilderson, T., Sirocko, F., 2000. Climate change and the collapse of the Akkadian empire: evidence from the deep sea. Geology 28, 379–382.

De Lange, G.J., Middelburg, J.J., Poorter, R.P., Shofiyah, S., 1989. Ferromanganese encrustations on the seabed west of Misool, eastern Indonesia. Neth. J. Sea Res. 24 (4), 541–553.

De Lange, G.J., van Santvoort, P.J.M., Langereis, C., Thomson, J., Corselli, C., Michard, A., Rossignol-Strick, M., Paterne, M., Anastasakis, G., 1999. Palaeo-environmental variations in eastern Mediterranean sediments: a multidisciplinary approach in a prehistoric setting. Progr. Oceanogr. 44, 369–386.

De Lange, G.J., Ten Haven, H.L., 1983. Recent sapropel formation in the eastern Mediterranean. Nature 305, 797–798.

De Lange, G.J., Thomson, J., Reitz, A., Slomp, C.P., Principato, M.S., Erba, E., Corselli, C., 2008. Synchronous basin-wide formation and redox-controlled preservation of a Mediterranean sapropel. Nat. Geosci. 1, 606–610.

De Rijk, S., Hayes, A., Rohling, E.J., 1999. Eastern Mediterranean sapropel S1 interruption: an expression of the onset of climatic deterioration around 7 ka BP. Mar. Geol. 153, 337–343.

Dimiza, M.D., Triantaphyllou, M.V., Dermitzakis, M.D., 2008. Seasonality and ecology of living coccolithophores in E. Mediterranean coastal environments (Andros Island, Middle Aegean Sea). Micropaleontology 54 (2), 159–175.

Ehrmann, W., Schmiedl, G., Hamann, Y., Kuhnt, T., Hemleben, C., Siebel, W., 2007. Clay minerals in late glacial and Holocene sediments of the northern and southern Aegean. Palaeogeogr., Palaeoclimatol., Palaeoecol. 249, 36–57.

Emeis, K.-C., Schulz, H., Struck, U., Rossignol-Strick, M., Erlenkeuser, H., Howell, M.W., Kroon, D., Mackensen, A., Ishizuka, S., Oba, T., Sakamoto, T., Koizumi, I., 2003. Eastern Mediterranean surface water temperatures and $\delta^{18}O$ composition during deposition of sapropels in the late Quaternary. Paleoceanography 18 (1), 1005. doi:10.1029/2000PA00061.

Emeis, K.C., Struck, U., Schulz, H.M., Rosenberg, R., Bernasconi, S., Erlenkeuser, H., Sakamoto, T., Martinez-Ruiz, F., 2000. Temperature and salinity variations of Mediterranean Sea surface waters over the last 16,000 years from records of planktonic stable oxygen isotopes and alkenone unsaturation ratios. Palaeogeogr., Palaeoclimatol., Palaeoecol. 158, 259–280.

Facorellis, Y., Maniatis, Y., Kromer, B., 1998. Apparent ^{14}C ages of marine mollusk shells from a Greek island: calculation of the marine reservoir effect in the Aegean Sea. Radiocarbon 40, 963–973.

Flores, J.A., Sierro, F.J., Francés, G., Vázquez, A., Zamarreño, I., 1997. The last 100,000 years in the western Mediterranean: sea surface water amd frontal dynamics as revealed by coccolithophores. Mar. Micropaleontol. 29, 351–366.

Flores, J.A., Barcena, M.A., Sierro, F.J., 2000. Ocean-surface and wind dynamics in the Atlantic Ocean off Northwest Africa during the last 140 000 years. Palaeogeogr., Palaeoclimatol., Palaeoecol. 161, 459–478.

Fontanier, C., Jorissen, F.J., Licari, L., Alexandre, A., Anschutz, P., Carbonel, P., 2002. Live benthic foraminiferal faunas from the Bay of Biscay: faunal density, composition, and microhabitats. Deep-Sea Res., Part 1, Oceanogr. Res. Pap. 49 (4), 751–785.

Friedrich, W.L., Kromer, B., Friedrich, M., Heinemeier, J., Pfeiffer, T., Talamo, S., 2006. Santorini eruption radiocarbon dated to 1627–1600 B.C. Science 312 (5773), 548.

Geraga, M., Tsaila-Monopoli, St., Ioakim, Ch., Papatheodorou, G., Ferentinos, G., 2000. An evaluation of paleoenvironmental changes during the last 18000 yr BP in the Myrtoon Basin, S.W. Aegean Sea. Paleogeogr., Palaeoclimatol., Palaeoecol. 156, 1–17.

Geraga, M., Tsaila-Monopolis, St., Ioakim, Ch., Papatheodorou, G., Ferentinos, G., 2005. Short-term climate changes in the southern Aegean Sea over the last 48.000 years. Paleogeogr., Palaeoclimatol., Palaeoecol. 220, 311–332.
Giunta, S., Negri, A., Morigi, C., Capotondi, L., Combourieu-Nebout, N., Emeis, K.C., Sangiorgi, F., Vigliotti, L., 2003. Coccolithiphorid ecostratigraphy and multiproxy paleoceanographic reconstruction in the Southern Adriatic Sea during the last deglacial time (Core AD91-17). Palaeogeogr., Palaeoclimatol., Palaeoecol. 190, 39–59.
Gogou, A., Bouloubassi, I., Lykousis, V., Arnaboldi, M., Gaitani, P., Meyers, P.A., 2007. Organic geochemical evidence of abrupt late Glacial–Holocene climate changes in the North Aegean Sea. Palaeogeogr., Palaeoclimatol., Palaeoecol. 256, 1–20.
Hamann, Y., Ehrmann, W., Schmiedl, G., Kruger, S., Stuut, J.-B., Kuhnt, T., 2008. Sedimentation processes in the Eastern Mediterranean Sea during the Late Glacial and Holocene revealed by end-member modelling of the terrigenous fraction in marine sediments. Mar. Geol. 248, 97–114.
Harris, P.G., Zhao, M., Rosell-Melé, A., Tiedemann, R., Sarnthein, M., Maxwell, J.R., 1996. Chlorin accumulation rate as a proxy for Quaternary marine primary productivity. Nature 383, 63–65.
Herbert, T.D., 2003. Alkenone paleotemperature determinations. In: Elderfield, H., Turekian, K.K. (Eds.), Chapter in Treatise in Marine Geochemistry. Elsevier, pp. 391–432.
Higgs, N.C., Thomson, J., Wilson, T.R.S., Croudace, I.W., 1994. Modification and complete removal of eastern Mediterranean sapropels by postdepositional oxidation. Geology 22 (5), 423–426.
Hilgen, H.J., 1991. Astronomical calibration of Gauss to Matuyama sapropels in the Mediterranean and implication for the geomagnetic polaritytime scale. Earth Planet. Sci. Lett. 104, 226–244.
Hilgen, F.J., Abdul Aziz, H., Krijgsman, W., Raffi, I., Turco, E., 2003. Integrated stratigraphy and astronomical tuning of the Serravallian and lower Tortonian at Monte dei Corvi (Middle–Upper Miocene, northern Italy). Palaeogeogr., Palaeoclimatol., Palaeoecol. 199, 229–264.
Hinrichs, K.-U., Schneider, R.R., Müller, P.J., Rullkötter, J., 1999. A biomarker perspective on paleoproductivity variations in two Late Quaternary sediment sections from the Southeast Atlantic Ocean. Org. Geochem. 30 (5), 341–366.
Incarbona, A., Di Stefano, E., Patti, B., Pelosi, N., Bonomo, S., Mazzola, S., Sprovieri, R., Tranchida, G., Zgozi, S., Bonanno, A., 2008. Holocene millennial-scale productivity variations in the Sicily Channel (Mediterranean Sea). Paleoceanography 23, PA3204. doi:10.1029/2007PA001581.
Jung, S.J.A., Davies, G.R., Ganssen, G.M., Kroom, D., 2004. Stepwise Holocene aridification in NE Africa deduced from dust-borne radiogenic isotope records. Earth Planet. Sci. Lett. 7031, 1–11.
Kemp, A.E.S., Pearce, R.B., Koizumi, I., Pike, J., Rance, S.J., 1999. The role of mat-forming diatoms in the formation of Mediterranean sapropels. Nature 398, 57–61.
Klok, J., Baas, M., Cox, H.C., de Leeuw, J.W., Schenck, P.A., 1984. Loliolides and dihydroactinidiolide in a recent marine sediment probably indicate a major tranformation pathway of carotenoids. Tetrahedron Lett. 25, 5577–5580.
Kornilova, O., Rosell-Mele, A., 2003. Application of microwave-assisted extraction to the analysis of biomarker climate proxies in marine sediments. Org. Geochem. 34, 1517–1523.
Kotthoff, U., Pross, J., Muller, U.C., Peyron, O., Schmiedl, G., Schultz, H., Bordon, A., 2008. Climate dynamics in the borderlands of the Aegean Sea during formation of sapropel S1 deduced from a marine pollen record. Quat. Sci. Rev. 27, 832–845.
Krom, M.D., Brenner, N.K., Neori, A., Gordon, L.I., 1992. Nutrient dynamics and new production in a warm-core eddy from the Eastern Mediterranean Sea. Deep-Sea Res. 39, 467–480.
Kuhnt, T., Schmiedl, G., Ehrmann, W., Hamann, Y., Hemleben, C., 2007. Deep-sea ecosystem variability of the Aegean Sea during the past 22 kyr as revealed by Benthic Foraminifera. Mar. Micropaleontol. 64, 141–162.
Lascaratos, A., 1992. Hydrology of the Aegean Sea. In: Charnock, H. (Ed.), Winds and Currents of the Mediterranean Basin, NATO Advanced Science Institute: Atmospheric and Oceanic Circulation in the Mediterranean Basin. Reports in Meteorology and Oceanography, vol. no. 40. Harvard University, pp. 313–334.
Lourens, L.J., Hilgen, F.J., Gudjonsson, L., Zachariasse, W.J., 1992. Late Pliocene to Early Pleistocene astronomically forced sea surface productivity and temperature variations in the Mediterranean. Mar. Micropaleontol. 19, 49–78.
Lourens, L.J.A., Antonarakou, F.J., Hilgen, F.J., Van Hoof, A.A.M., Vergnaud-Grazzini, C., Zachariasse, W.J., 1996. Evaluation of the Plio–Pleistocene astronomical timescale. Paleoceanography 11, 391–431.
Lykousis, V., Chronis, G., Tselepides, A., Price, N.B., Theocharis, A., Siokou-Fragou, I., van Wambeke, F., Danovaro, R., Stavrakakis, S., Duineveld, G., Georgopoulos, D., Ignatiades, L., Souvermezoglou, A., Voutsinou-Taliadouri, F., 2002. Major outputs of the recent multidisciplinary biogeochemical researches undertaken in the Aegean Sea. J. Mar. Syst. 33–34, 313–334.
Marino, G., 2008. Paleoceanography of the interglacial eastern Mediterranean Sea. LPP Foundation Utrecht, Contribution Series, vol. 24. 145 pp.
Marino, G., Rohling, E.J., Rijpstra, W.I., Sangiorgi, F., Schouten, S., Sinninghe Damsté, J.S., 2007. Aegean Sea as driver of hydrological and ecological changes in the eastern Mediterranean. Geology 35, 675–678.
Marlowe, I.T., Green, J.C., Neal, A.C., Brassell, S.C., Eglinton, G., Course, P.A., 1984. Long chain (*n*-C37–C39) alkenones in the Prymnesiophyceae. Distribution of alkenones and other lipids and their taxonomic significance. Br. Phycol. J. 19, 203–216.
Mayewski, P.A., Rohling, E., Stager, C.J., Karlen, W., Maasch, K.A., Meeker, L.D., Meyerson, E.A., Gasse, F., van Kreveld, S., Holmgren, K., Lee-Thorp, J., Rosqvist, G., Rack, F., Staubwasser, M., Schneider, R.R., Steig, E., 2004. Holocene climate variability. Quat. Res. 62, 243–255.
McManus, J., Berelson, W.M., Klinkhamme, G.P., Johnson, K.S., Coale, K.H., Anderson, R.F., Kumar, N., Buridge, D.J., Hammond, D.E., Brumsack, H.J., McCorkle, D.C., Rusdi, A., 1998. Geochemistry of barium in marine sediments: implications for its use as a paleoproxy. Geochim. Cosmochim. Acta 62, 3453–3473.
Menzel, D., Hopmans, E.C., van Bergen, P.F., de Leeuw, J.W., Sinninghe Damste, J.S., 2002. Development of photic zone euxinia in the eastern Mediterranean Basin during deposition of Pliocene sapropels. Mar. Geol. 189, 215–226.
Menzel, D., van Bergen, P.F., Schouten, S., Sinninghe Damste, J.S., 2003. Reconstruction of changes in export productivity during Pliocene sapropel deposition: a biomarker approach. Palaeogeogr., Palaeoclimatol., Palaeoecol. 190, 273–287.
Mercone, D., Thomson, J., Croudace, I.W., Siani, G., Paterne, M., Troelstra, S., 2000. Duration of S1, the most recent sapropel in the eastern Mediterranean Sea, as indicated by AMS radiocarbon and geochemical evidence. Paleoceanography 15, 336–347.
Mercone, D., Thomson, J., Abu-Zied, R.H., Croudace, I.W., Rohling, E.J., 2001. High-resolution geochemical and micropaleontological profiling of the most recent eastern Mediterranean sapropel. Mar. Geol. 177, 25–44.
Migowski, C., Mordechai, S., Prasad, S., Negendank, J.F.W., Agnon, A., 2006. Holocene climate variability and cultural evolution in the Near East from the Dead Sea sedimentary record. Quat. Res. 66, 421–431.
Molfino, B., McIntyre, A., 1990. Precessional forcing of nutricline dynamics in the Equatorial Atlantic. Science 249, 766–769.
Moodley, L., Middelburg, J.J., Herman, P.M.J., Soetaert, K., de Lange, G.J., 2005. Oxygenation and organic-matter preservation in marine sediments: direct experimental evidence from ancient organic carbon-rich deposits. Geology 33, 889–892.
Mudie, P.J., Rochon, A., Aksu, A.E., 2002. Pollen stratigraphy of Late Quaternary cores from Marmara Sea: land–sea correlation and paleoclimatic history. Mar. Geol. 190, 233–260.
Muller, P.J., Kirst, G., Ruhland, G., von Storch, L., Rosell-Mele, A., 1998. Calibration of the alkenone paleotemperature index Uk37 based on core tops from the eastern South Atlantic and the global ocean (60°N–60°S). Geochim. Cosmochim. 62, 1757–1772.
Negri, A., Giunta, S., 2001. Calcareous nannofossil paleoecology in the sapropel S1 of the eastern Ionian sea: paleoceanographic implications. Palaeogeogr., Palaeoclimatol., Palaeoecol. 169, 101–112.
Okada, H., Honjo, S., 1973. The distribution of ocean coccolithophorids in the Pacific. Deep-Sea Res. 20, 355–374.
Papanikolaou, D., Nomikou, P., 2001. Tectonic structure and volcanic centres at the eastern edge of the Aegean Volcanic Arc around Nisyros Island. Bull. Geol. Soc. Greece 34 (1), 289–296.
Parker, A.G., Goudie, A.S., Stokes, S., White, K., Hodson, M.J., Manning, M., Kennet, D., 2006. A record of Holocene climate change from lake geochemical analyses in southeastern Arabia. Quat. Res. 66, 465–476.
Pavlopoulos, K., Karkanas, P., Triantaphyllou, M., Karymbalis, E., Tsourou, T., Palyvos, N., 2006. Paleoenvironmental evolution of the coastal plain of Marathon, Greece, during the Late Holocene: depositional environment, climate, and sea level changes. J. Coast. Res. 22, 424–438.
Perissoratis, C., Piper, D.J.W., 1992. Age, regional variation, and shallowest occurrence of S1 sapropel in the Northern Aegean Sea. Geo-Mar. Lett. 12, 49–53.
Poulos, S.E., Drakopoulos, P.G., Collins, M.B., 1997. Seasonal variability in sea surface oceanographic conditions in the Aegean Sea (Eastern Mediterranean): an overview. J. Mar. Syst. 13, 225–244.
Principato, M., Crudeli, D., Ziveri, P., Slomp, C.P., Corselli, C., Erba, E., de Lange, G.J., 2006. Phyto- and zooplankton paleofluxes during the deposition of sapropel S1 (eastern Mediterranean): biogenic carbonate preservation and paleoecological implications. Palaeogeogr., Palaeoclimatol., Palaeoecol. 235, 8–27.
Principato, M., Giunta, S., Corselli, C., Negri, A., 2003. Late Pleistocene–Holocene planktonic assemblages in three box-cores from the Mediterranean Ridge area (west-southwest of Crete): paleoecological and palaeoceanographic reconstruction of sapropel S1 interval. Palaeogeogr., Palaeoclimatol., Palaeoecol. 190, 61–77.
Reimer, P.J., McCormac, F.G., 2002. Marine radiocarbon reservoir corrections for the Mediterranean and Aegean Seas. Radiocarbon 44 (1), 159–166.
Reitz, A., Thomson, J., De Lange, G.J., Green, D.R.H., Slomp, C.P., Gebhardt, A.C., 2006. Effects of the Santorini (Thera) eruption on manganese behaviour in Holocene sediments of the eastern Mediterranean. Earth Planet. Sci. Lett. 241, 188–201.
Repeta, D.J., 1989. Carotenoid diagenesis in recent marine sediments. II. Degradation of fucoxanthin to loliolide. Geochim., Cosmochim. 53, 699–707.
Robinson, S.A., Black, S., Sellwood, B.W., Valdes, P.J., 2006. A review of paleoclimates and paleoenvironments in the Levant and eastern Mediterranean from 25000 to 5000 years BP: setting the environmental background for the evolution of human civilisation. Quat. Sci. Rev. 25, 1517–1541.
Roether, W., Manca, B.B., Klein, B., Bregant, D., Georgopoulos, D., Beitzel, V., Kovačević, V., Luchetta, A., 1996. Recent changes in eastern Mediterranean deep waters. Science 271, 333–335.
Rohling, E.J., Sprovieri, M., Cane, T., Casford, J.S.L., Cooke, S., Bouloubassi, I., Emeis, K.C., Schiebel, R., Rogerson, M., Hayes, A., Jorissen, F.J., Kroon, D., 2004. Reconstructing past planktic foraminiferal habitats using stable isotope data: a case history for Mediterranean sapropel S5. Mar. Micropaleontol. 50 (1–2), 89–123.
Rohling, E.J., Jorissen, F.J., De Stigter, H.C., 1997. 200 Year interruption of Holocene sapropel formation in the Adriatic Sea. J. Micropalaeontol. 16 (2), 97–108.
Rohling, E.J., Mayewski, P.A., Abu-Zied, R.H., Casford, J.S.L., Hayes, A., 2002b. Holocene atmosphere–ocean interactions: records from Greenland and The Aegean Sea. Clim. Dyn. 18, 587–593.
Rohling, E.J., 1994. Review and new aspects concerning the formation of eastern Mediterranean sapropels. Mar. Geol. 122, 1–28.
Rohling, E.J., Cane, T.R., Cooke, S., Sprovieri, M., Bouloubassi, I., Emeis, K.C., Schiebel, R., Kroon, D., Jorissen, F.J., Lorre, A., Kemp, A.E.S., 2002a. African monsoon variability during the previous interglacial maximum. Earth Planet. Sci. Lett. 202, 61–75.
Rohling, E.J., Gieskes, W.W.C., 1989. Late Quaternary changes in Mediterranean intermediate water density and formation rate. Paleoceanography 4, 531–545.

Rossignol-Strick, M., 1995. Sea–land correlation of pollen records in the Eastern Mediterranean for the Glacial–Interglacial transition: biostratigraphy versus radiometric time-scale. Quat. Sci. Rev. 14, 893–915.
Rossignol-Strick, M., Nesteroff, W., Olive, P., Vergnaud-Grazzini, C., 1982. After the deluge: Mediterranean stagnation and sapropel formation. Nature 295, 105–110.
Roussakis, G., Karageorgis, A.P., Conispoliatis, N., Lykousis, V., 2004. Last glacial–Holocene sediment sequences in N. Aegean basins: structure, accumulation rates and clay mineral distribution. Geo-Mar. Lett. 24, 97–111.
Sangiorgi, F., Capotondi, L., Nebout, N.C., Vigkiotti, L., Brinkhuis, H., Giounta, S., Lotter, A.F., Morigi, C., Negri, A., Reichart, G.-J., 2003. Holocene seasonal sea-surface temperature variation in the southern Adriatic Sea inferred from a multiproxy approach. J. Quat. Sci. 18, 723–732.
Scrivner, A.E., Vance, D., Rohling, E.J., 2004. New neodymium isotope data quantify Nile involvement in Mediterranean anoxic episodes. Geology 32, 565–568.
Sinninghe Damsté, J.S., Rijpstra, W.I.C., Reichart, G.J., 2002. The influence of oxic degradation on the sedimentary biomarker record II. Evidence from Arabian Sea sediments. Geochim., Cosmochim. 66, 2737–2754.
Slomp, C.P., Thomson, J., De Lange, G.J., 2004. Controls on phosphorus regeneration and burial during formation of eastern Mediterranean sapropels. Mar. Geol. 203, 141–159.
Sperling, M., Schmiedl, G., Hemleben, Ch., Emeis, K.C., Erlenkeuser, H., Grootes, P.M., 2003. Black Sea impact on the formation of eastern Mediterranean sapropel S1? Evidence from the Marmara Sea. Palaeogr., Palaeoclimatol., Palaeoecol. 190, 9–21.
Stavrakakis, S., Chronis, G., Tselepides, A., Heussner, S., Monaco, A., Abassis, A., 2000. Downward fluxes of settling particles in the deep Cretan Sea (NE Mediterranean). Progr. Oceanogr. 46, 217–240.
Stratford, K., Williams, R.G., Myers, P.G., 2000. Impact of the circulation on sapropel formation in the eastern Mediterranean. Glob. Biogeochem. Cycles 14, 683–695.
Stuiver, M., Reimer, P.J., Bard, E., Beck, J.W., Burr, G.S., Hughen, K.A., Kromer, B., McCormac, G., Van Der Plicht, J., Spurk, M., 1998. INTCAL98 radiocarbon age calibration, 24,000–0 cal BP. Radiocarbon 40 (3), 1041–1083.
Stuiver, M., Reimer, P.J., 1993. Extended C-14 data-base and revised Calib 3.0 C-14 age calibration program. Radiocarbon 35, 215–230.
Targarona, J., 1997. Climatic and oceanographic evolution of the Mediterranean region over the last glacial–interglacial transition. Laboratory of Palaeobotany and Palynology: LPP Contribution series, vol. no 7. Utrecht, 155 pp.
Ternois, Y., Sicre, M.-A., Boireau, A., Marty, J.-C., Miquel, J.-C., 1996. Production pattern of alkenones in the Mediterranean Sea. Geophys. Res. Lett. 23 (22), 3171–3174.
Theocharis, A., Nittis, H., Kontoyiannis, E., Papageorgiou, E., Balopoulos, E., 1999. Climatic changes in the Aegean Sea influence the Eastern Mediterranean thermohaline circulation (1986–1997). Geophys. Res. Lett. 26 (11), 1617–1620.
Thomson, J., Mercone, D., De Lange, G.J., Van Santvoort, P.J.M., 1999. Review of recent advances in the interpretation of eastern Mediterranean sapropel S1 from geochemical evidence. Mar. Geol. 153 (1–4), 77–89.
Tolun, L., Çağatay, M.N., Carrigan, W.J., 2002. Organic geochemistry and origin of Late Glacial–Holocene sapropelic layers and associated sediments in Marmara Sea. Mar. Geol. 190, 47–60.
Triantaphyllou, M.V., Ziveri, P., Tselepides, A., 2004. Coccolithophore export production and response to seasonal surface water variability in the oligotrophic Cretan Sea (NE Mediterranean). Micropaleontology 50, 127–144.
Tselepides, A., Zervakis, V., Polychronaki, T., Danovaro, R., Chronis, G., 2000. Distribution of nutrients and particulate organic matter in relation to the prevailing hydrographic features of the Cretan Sea (NE Mediterranean). Progr. Oceanogr. 46, 113–142.
Van Os, B.J.H., Lourens, L.J., Hilgen, F.J., de Lange, G.J., Beaufort, L., 1994. The formation of Pliocene sapropels and carbonate cycles in the Mediterranean: diagenesis, dilution, and productivity. Paleoceanography 9, 601–617.
Vermoere, M., Degryse, P., Vanhecke, L., Muchez, Ph., Paulissen, E., Smets, E., Waelkens, M., 1999. Pollen analysis of two travertine sections in Baskoy (southwestern Turkey): implications for environmental conditions during the early Holocene. Review of Palaeobotany and Palynology 105, 93–110.
Versteegh, G.J.M., Zonneveld, K.A.F., 2002. Use of selective degradation to separate preservation from productivity. Geology 30 (7), 615–618.
Volkman, J.K., Barrett, S.M., Blackburn, S.I., 1999. Eustigmatophyte microalgae potential sources of C_{29} sterols, C_{22}–C_{28} *n*-alcohols and C_{28}–C_{32} *n*-alkyl diols in freshwater environments. Org.Geochem. 30, 307–318.
Von Breymann, M.T., Emeis, K.C., Suess, E., 1992. Water-depth and diagenetic constraints in the use of barium as a paleoproductivity indicator. In: Summerhayes, C.P., Prell, W., Emeis, K.C. (Eds.), Evolution of Upwelling Systems since the Early Miocene: Geol. Soc. Lond. Spec. Publ., vol. 64, pp. 273–284.
Weiss, H., Courty, M.-A., Wetterstrom, W., Meadow, R., Senior, L., Guichard, F., Curnow, A., 1993. The genesis and collapse of third millennium north Mesopotamian civilization. Science 261, 995–1004.
Winter, A., Jordan, R.W., Roth, P., 1994. Biogeography of living Coccolithophores in oceanic waters. In: Winter, A., Siesser, W.G. (Eds.), Coccolithophores. Cambridge University Press, pp. 13–27.
Young, J.R., 1994. Functions of coccoliths. In: Winter, A., Siesser, W.G. (Eds.), Coccolithophores. Cambridge University Press, pp. 63–82.
Yüce, H., 1995. Northern Aegean Water Masses. Estuar., Coast. Shelf Sci. 41 (3), 325–343.
Zervakis, V., Georgopoulos, D., Drakopoulos, P.G., 2000. The role of the North Aegean in triggering the recent Eastern Mediterranean climatic changes. J. Geophys. Res. 105, 26103–26116.
Zervakis, V., Georgopoulos, D., Karageorgis, A.P., Theocharis, A., 2004. On the response of the Aegean sea to climatic variability: a review. Int. J. Climatol. 24, 1845–1858.
Ziveri, P., Baumann, K.H., Böckel, B., Bollmann, J., Young, J., 2004. Biogeography of selected coccolithophores in the Atlantic Ocean, from Holocene sediments. In: Thierstein, H., Young, J. (Eds.), Coccolithophores: From Molecular Processes to Global Impact. Springer Verlag, pp. 403–428.